

Metal–metal and metal–ligand bond strengths in metal carbonyl clusters

Andrew K. Hughes, Ken Wade *

Chemistry Department, Durham University, Science Laboratories, South Road, Durham DH1 3LE, UK

Received 13 April 1999; accepted 21 July 1999

Dedicated to Professor Ron J. Gillespie FRS on the occasion of his 75th birthday, when despite those years he continues so effectively to shed fresh light and understanding on all he touches, providing new insight (and demolishing cherished myths) on a variety of fundamental chemical topics with a vigour envied by those half his age. We hope this present exploration of patterns lurking in the literature on metal cluster structures and bonding catches the spirit of what Ron himself does so well.

Contents

Abstract	191
1. Introduction	192
2. The method: bond length/bond enthalpy relationships	193
3. Metal carbonyls of known heats of formation: metal–ligand bond enthalpies	197
4. Neutral osmium clusters, $\text{Os}_x(\text{CO})_y$	200
5. Osmium carbonyl anions $[\text{Os}_x(\text{CO})_y]^{2-}$ and hydrides $[\text{Os}_x(\text{CO})_y\text{H}_z]^{c-}$; further characteristics of osmium carbonyl clusters	206
6. Osmium carbonyl carbide clusters, $[\text{Os}_x(\text{CO})_y\text{H}_x\text{C}]^{c-}$	214
7. Rhenium carbonyl clusters, $[\text{Re}_x(\text{CO})_y\text{H}_z]^{c-}$ and $[\text{Re}_x(\text{CO})_y\text{H}_z\text{C}]^{c-}$	215
8. Rhodium carbonyl clusters, $[\text{Rh}_x(\text{CO})_y\text{H}_z]^{c-}$ and $[\text{Rh}_x(\text{CO})_y\text{H}_z\text{E}]^{c-}$	219
9. Metal carbides	221
10. Conclusions.	225
Acknowledgements	227
References	227

Abstract

The limited experimental thermochemical information about metal carbonyl clusters, and the more extensive literature on structural studies of such compounds, provide a means of

* Corresponding author. Tel.: +44-191-3743-111; fax: +44-191-3861-127.

E-mail address: kenneth.wade@durham.ac.uk (K. Wade)

exploring trends in their stabilities. This review surveys that literature for selected metals, showing how the enthalpy of disruption of gaseous $M_x(CO)_y$ clusters into gaseous metal atoms and carbon monoxide can be partitioned into two components representing the strengths of metal–metal and metal–ligand bonds. In doing so, it is assumed that the bond enthalpies, $E(M-M)$, of metal–metal bonds vary smoothly with their length, $d(M-M)$, according to a relationship $E(M-M) = A[d(M-M)]^{-4.6}$, for which a justification is provided. The structure of a cluster thus provides a means of determining the total metal–metal bond enthalpy of that cluster. Application of this method to thermodynamically characterised clusters demonstrates that the average metal–ligand bond enthalpy, $E(M-CO)$, in carbonyl clusters $M_x(CO)_y$, varies slightly with the ligand to metal ratio, y/x ; a carbonyl ligand binds more strongly to a metal when it is competing with few other ligands. We demonstrate that for binary osmium carbonyl clusters, $Os_x(CO)_y$, the distances $d(Os-C)$ and $d(C-O)$ are also functions of the ligand to metal ratio, y/x , providing evidence for the familiar synergistic bonding of the carbonyl ligand, and that these distances are a function of the metal–ligand bond enthalpy, $E(Os-CO)$. Trends in cluster stability, as determined by the total metal–metal bond enthalpy, $\Sigma E(M-M)$, for anionic and carbonyl hydride clusters of osmium, rhenium and rhodium, $[M_x(CO)_yH_z]^{e-}$, are presented. Similar trends for clusters of rhenium and rhodium containing core or interstitial carbon, nitrogen or other atoms are also explored, and partition of the atomisation enthalpy of binary metal carbides, MC and M_2C , into metal–metal and metal–carbon components is investigated to provide insight into the strength of binding of core carbon atoms surrounded by octahedral arrays of metal atoms. © 2000 Elsevier Science S.A. All rights reserved.

Keywords: Metal carbonyl clusters; Metal–metal bond enthalpies; Metal–ligand bond enthalpies

1. Introduction

Metal carbonyl cluster chemistry, indeed metal cluster chemistry in general, is an area that is now well documented structurally [1–3]. Many individual papers and review articles have discussed the various ways in which the shapes of cluster molecules can be interpreted, often predicted, in terms of the numbers of electrons available for bonding, whether in terms of 2- and occasionally 3-centre electron pair bonds and the 18-electron rule as a means of understanding the numbers of contacts between their skeletal atoms [4], or in terms of the overall numbers of skeletal electron pairs available to hold their skeletal polyhedra together [5–7]. Despite our now relatively sophisticated understanding of their shapes, and of the links between shapes and electron numbers, our understanding of the *strengths* of the metal–metal and metal–ligand bonds they contain, and of the relative efficiencies with which different clusters make use of the electrons formally available for bonding, remains limited. This is partly because only limited thermochemical data are available [8,9], and partly because few attempts have been made to explore what trends can be perceived in those data. The purpose of this present survey is:

1. to draw attention to trends that readily become apparent when structural and thermochemical data are pooled;
2. to show in what areas it would be helpful to collect more thermochemical data to flesh out the picture that we believe is emerging, and
3. to make some thermochemical predictions from structural data.

In principle, carbonyl complexes are particularly suited to such tasks, because of the familiar π -acidic nature of the carbonyl ligand. Free (gaseous) carbon monoxide is held together by a carbon–oxygen triple bond, and has a lone pair of electrons available for donation to a suitable Lewis acid on both the oxygen and the carbon atoms. The latter, being on the less electronegative atom, is the pair of electrons through which carbon monoxide normally forms a σ -bond to a proton, a metal atom, or some other Lewis acid residue. If that Lewis acid residue contains non-bonding (or weakly bonding) electrons in p- or d-orbitals orientated appropriately for back π -bonding to the π^* orbital of the CO ligand, Fig. 1, such π -bonding can strengthen the bond between the ligand carbon atom and the acceptor atom, though at the expense of a weakened carbon–oxygen bond in the ligand. This effect is reflected in the familiar reduction in $\nu(\text{CO})$ when carbon monoxide coordinates to an acceptor atom capable of such back π -bonding, though the effect is complicated by vibrational coupling even in quite simple molecules [10]. It is also reflected in the carbon–oxygen bond distances, $d(\text{C–O})$, in carbonyl complexes, which lengthen progressively as more electron density is shifted into the ligand π^* orbitals. However, because of the short length and high bond order (and strength) of the carbon–oxygen bonds concerned, the changes in $d(\text{C–O})$ on coordination are small and have rarely been measured with sufficient precision to allow detailed quantitative interpretation of these subtle changes. Nevertheless we show below that crude correlations can already be drawn between ligand carbon–oxygen distances and cluster nuclearity which we believe reflect changing degrees of back π -bonding from metal atoms to ligands. Such correlations will be tested and made more precise in future as solid-state structures are determined progressively more accurately.

2. The method: bond length/bond enthalpy relationships

Published thermochemical data on metal carbonyl cluster compounds $\text{M}_x(\text{CO})_y$ and related systems have typically been derived from micro-calorimetric measurements of enthalpies of combustion or other oxidative reactions [8,9]. From these one can calculate enthalpies of formation, $\Delta_f H$, and of disruption into gaseous metal atoms and carbon monoxide molecules, ΔH_{dis} , using published enthalpies of formation of these gaseous species:

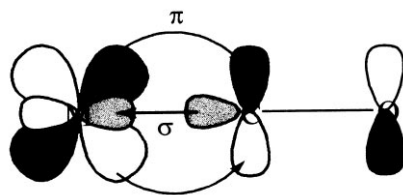
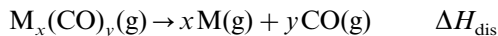


Fig. 1. The σ - and π -bonding modes of a metal carbonyl ligand.



$$\Delta H_{\text{dis}} = x\Delta_f H^\circ[\text{M}](\text{g}) + y\Delta_f H^\circ(\text{CO})(\text{g}) - \Delta_f H^\circ[\text{M}_x(\text{CO})_y](\text{g})$$

Assuming that the disruption enthalpy can be partitioned between two terms, the enthalpy change associated with the cleavage of all the metal–metal bonds, $\Sigma E(\text{M}–\text{M})$, and that associated with cleavage of the metal–ligand bonds, $\Sigma E(\text{M}–\text{CO})$, one can write

$$\Delta H_{\text{dis}} = \Sigma E(\text{M}–\text{M}) + \Sigma E(\text{M}–\text{CO})$$

It is on the first of these terms, $\Sigma E(\text{M}–\text{M})$, that we shall focus primarily in the present survey. We outline a method by which metal–metal bond energy terms, $E(\text{M}–\text{M})$, can be calculated from bond lengths, $d(\text{M}–\text{M})$, for metal cluster compounds in general, simply by assuming that the metal–metal bonds in metal clusters resemble those in the bulk metal and conform to the same length–energy relationship. Having made that assumption, and calculated the total strength, $\Sigma E(\text{M}–\text{M})$, of the metal–metal bonds in specific clusters, we show how that varies with the numbers of electrons provided by the ligands and, for cluster compounds whose enthalpies of formation have been experimentally determined, we show how the strengths of the metal–ligand bonds can also be deduced.

At the heart of our treatment is the assumption that the shorter a bond is between two specified atoms, the stronger it is [11,12]. This is the basis of the Bond Valence method in extended solids [13,14], and is demonstrably true for covalent compounds in general for which structural and thermochemical data are available [15,16], and in particular for organic compounds for which heats of formation can be calculated by summing bond enthalpy terms that in themselves reflect bond orders and so lengths [17]. Typical values for bonds involving carbon atoms are 348 kJ mol^{−1} for a carbon–carbon single bond (length 154 pm), 612 kJ mol^{−1} for a carbon=carbon double bond (length 134 pm), and 837 kJ mol^{−1} for a carbon≡carbon triple bond (length 120 pm) [18]. Corresponding values for carbon–oxygen bond enthalpies are C–O, 143 pm, 360 kJ mol^{−1}; C=O, 122 pm, 743 kJ mol^{−1}; C≡O, 112.8 pm [19], 1076 kJ mol^{−1}.

Where bonds of intermediate bond orders have to be considered, as in aromatic systems, it is convenient to express the bond enthalpies, $E(\text{C}–\text{X})$, in terms of their lengths, $d(\text{C}–\text{X})$, in the form of a relationship

$$E = A d^{-k}$$

where A and k are constants for a particular bond type; plots of $\log(E)$ against $\log(d)$ are linear of slope $-k$ and intercept $\log(A)$. We use a relationship of this type in the present work, to calculate metal–metal bond enthalpies, $E(\text{M}–\text{M})$, from their lengths, $d(\text{M}–\text{M})$. The advantage of such a relationship is that it requires only two constants, A and k , and relates strength to length without requiring that the bond order be determined.

The values of A and k , the constants for a particular bond type that allow individual bond enthalpies to be calculated for bonds involving a particular metal M , have been deduced from structural and thermochemical measurements on the

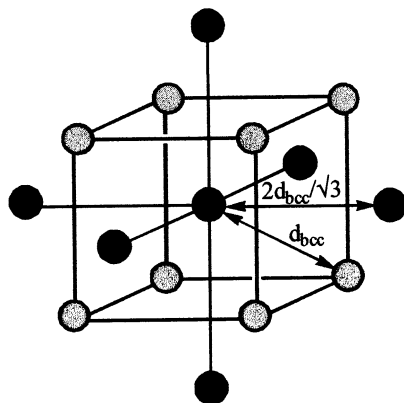


Fig. 2. The bcc lattice, drawn to emphasise the 14 coordination of each atom. Comprised of eight atoms at the corners of a cube (distance d_{bcc} pm), and six next-nearest neighbours at the corners of an octahedron (distance a pm, a = unit cell length = $2 d_{\text{bcc}}/\sqrt{3}$).

bulk metals. The parameter A , which determines the actual strength of a bond of specified length, varies markedly from metal to metal. However, the exponent k , which reflects the rate at which bond strengths vary with length, appears not to vary markedly from metal to metal. This can be shown by considering metals capable of crystallising in both a close-packed (cp) lattice (hexagonal close-packed, hcp, or face centred cubic, fcc) and a body centred cubic (bcc) lattice, with essentially the same enthalpy of atomisation, ΔH_{atom} . Vaporisation of a cp lattice, in which each metal atom is surrounded by 12 nearest neighbours at a distance d_{cp} , requires on average six such M–M bonds to be cleaved to liberate one metal atom. Hence

$$\Delta H_{\text{atom}} = 6 E(\text{M–M})_{\text{cp}}$$

We should stress that in referring to metal–metal ‘bonds’ we are not referring to classical electron pair bonds, and are not as a basis making any assumptions about the numbers of electrons available for bonding in bulk metals, or about their distribution. Rather, we are assuming that in a close packed lattice all 12 of the pairwise links between neighbouring atoms are bonding, and we deduce their strength from the enthalpy change when all such links are broken, as when the bulk metal is vaporised to form a monatomic gas.

In a body centred cubic lattice each metal atom is immediately surrounded by eight nearest neighbours at a distance d_{bcc} , and by six more arranged octahedrally at a distance $2 d_{\text{bcc}}/\sqrt{3}$, i.e. $1.155 d_{\text{bcc}}$, through the cube faces, that effectively complete the coordination sphere of 14 atoms in total, see Fig. 2. These two types of bond in the coordination sphere will have bond enthalpies $E(\text{M–M})_{\text{bcc}}$ and $E'(\text{M–M})_{\text{bcc}}$ which reflect their lengths, d_{bcc} and $1.155 d_{\text{bcc}}$, and on average four of the former type and three of the latter need to be broken per atom vaporised. Thus,

$$\Delta H_{\text{atom}} = 4 E(\text{M–M})_{\text{bcc}} + 3 E'(\text{M–M})_{\text{bcc}}$$

Expressing these bond enthalpies as a function of bond lengths, d , we obtain:

$$\Delta H_{\text{atom}} = 6 A [d_{\text{cp}}]^{-k} = 4 A [d_{\text{bcc}}]^{-k} + 3 A [2 d_{\text{bcc}}/\sqrt{3}]^{-k}$$

for metal atoms with essentially the same atomisation enthalpy for both close-packed and body centred cubic lattices.

Interestingly, for such metals, the ratio of $d_{\text{cp}}/d_{\text{bcc}}$ (the relative lengths of the bonds to nearest neighbour atoms in the close-packed and body centred cubic lattices) varies remarkably little from metal to metal, being for example 1.0177 for Ti, 1.0172 for Cr and 1.0171 for Fe. Even alkali and alkaline earth metals have similar ratios of $d_{\text{cp}}/d_{\text{bcc}}$ of ca. 1.018. We infer from the consistency of these ratios that the bonds in these metals are varying in strength with length at about the same rate, i.e. that the exponent k which reflects that rate does not vary markedly from metal to metal. Taking $d_{\text{cp}} = 1.017 d_{\text{bcc}}$ leads to the conclusion that $k = 4.6$, and it is this figure that we have used in calculating bond enthalpies $E(\text{M-M})$ from bond lengths, $d(\text{M-M})$, in the present work.

$$E(\text{M-M}) = A d(\text{M-M})^{-4.6}$$

Experimentally determined atomisation enthalpies, ΔH_{atom} , and interatomic distances, $d(\text{M-M})$, to nearest neighbour atoms in the bulk metal have been used to calculate the values of A for different transition metals. The data are summarised in Table 1 for the transition metals in the groups headed by the elements titanium to nickel. Note that although titanium, zirconium and hafnium preferentially crystallise in hcp lattices, for which the nearest neighbour bond enthalpies $E(\text{M-M})_{\text{cp}}$ are obtained by dividing ΔH_{atom} by six, the metals of the vanadium and chromium groups preferentially crystallise in bcc forms, and for these metals one needs to divide the atomisation enthalpy, ΔH_{atom} , by 5.55 (not four as is still used in some treatments) to determine the bond enthalpies, $E(\text{M-M})_{\text{bcc}}$ of their nearest neighbour bonds. The bond enthalpies $E'(\text{M-M})_{\text{bcc}}$ of the six next nearest neighbour bonds that complete the coordination sphere of 14 atoms in a bcc lattice are obtained by dividing ΔH_{atom} by 10.76 (the values 5.55 and 10.76 reflect the use of $k = 4.6$ for the exponent relating length to strength).

Table 1 shows that for the transition metal groups headed by the elements manganese (which itself forms a large number of metallic phases, none of which has an idealised regular lattice), iron and cobalt, the preferred structure for the first row metal differs from that for the heavier metals, though all three elements of the nickel group crystallise with face centred cubic lattices.

In the present survey we shall be concerned mainly with compounds of rhenium and of the iron and cobalt groups (notably osmium and rhodium), and we shall show how useful insight can be gained into the cluster chemistry of these transition metals by noting how the bonds in the bulk metals vary in strength with length and exploring the implications for other metal-metal bonded systems containing these and other metals. Throughout, we shall assume that the bond enthalpies $E(\text{M-M})$ in cluster compounds of these metals can be calculated from their lengths $d(\text{M-M})$ using the relationship $E(\text{M-M}) = A d(\text{M-M})^{-4.6}$, where A has the value characteristic of the particular element, as listed in Table 1.

3. Metal carbonyls of known heats of formation: metal–ligand bond enthalpies

There is a dearth of information on the thermochemistry of metal carbonyl clusters. During the past twenty years, during which there has been a dramatic growth in the numbers of metal carbonyl clusters that have been prepared and structurally characterised, very few measurements have been made of the heats of combustion or other reactions of such compounds from which to calculate their heats of formation [20]. In order to relate our discussion initially to systems of known thermochemistry, we are therefore restricted to a series of neutral metal carbonyl clusters first discussed in 1977 [8a] and 1978 [21,22] from which, however, enough features of the structure/energetics pattern could be discerned to encourage further work [23].

Table 2, which is adapted from Ref. [22], gives structural and thermochemical data for the metals of the iron and cobalt groups and those neutral carbonyl complexes of these metals on which thermochemical studies had been carried out before 1978, from which enthalpies of disruption into gaseous metal atoms and carbon monoxide molecules were calculated:

Table 1

The structures (bcc, hcp or fcc), enthalpies of atomisation, $\Delta_f H^\circ M(g)$ (kJ mol⁻¹), metal–metal bond lengths, $d(M-M)$ (pm), bond enthalpies of the individual M–M bonds [$E(M-M) = \Delta_f H^\circ/6$ or $\Delta_f H^\circ/5.55$ as appropriate], and resulting length–energy correlation constants A ($= E/d^{-4.6}$) $\times 10^{-13}$ for the metals of Groups 4–10^a

Symbol	Ti	V	Cr (α)	Mn ^c (α)	Fe (α)	Co (α)	Ni
Structure	hcp	bcc ^b	bcc	bcc	bcc	hcp	fcc
$\Delta_f H^\circ M(g)$	469.9	514.2	396.6	280.7	416.3	424.6	429.7
$d(M-M)$	289.56	262.24	249.80	266.79 (δ)	248.23	250.61	249.16
$E(M-M)$	78.3	92.7	71.6	51.3	75.1	71.4	71.5
A	1.651	1.239	0.766	0.742	0.780	0.774	0.756
Symbol	Zr	Nb	Mo	Tc	Ru	Rh	Pd
Structure	hcp	bcc	bcc	hcp	hcp	fcc	fcc
$\Delta_f H^\circ M(g)$	608.8	725.9	658.1	677.8	642.6	556.9	378.2
$d(M-M)$	317.9	285.84	272.51	270.3	265.02	269.01	275.11
$E(M-M)$	101.5	130.2	118.4	115.8	108.5	92.9	62.1
A	3.288	2.587	1.888	1.780	1.522	1.396	1.034
Symbol	Hf	Ta	W	Re	Os	Ir	Pt
Structure	hcp	bcc	bcc	hcp	hcp	fcc	fcc
$\Delta_f H^\circ M(g)$	619.2	782.0	849.3	769.8	790.7	665.2	565.3
$d(M-M)$	312.73 (α)	286	274.09	274.1	267.54	271.4	274.9
$E(M-M)$	103.2	141.7	153.8	129.3	131.6	110.9	94.6
A	3.100	2.823	2.519	2.188	1.929	1.735	1.571

^a Structural data and enthalpy of atomisation were taken from the CRC Handbook of Chemistry and Physics, D.R. Lide (Ed.), 72nd ed., CRC Press, Boca Raton.

^b For the metals with bcc structure, the metal–metal bond length quoted is the 8-coordinate distance, for the fcc and hcp metals the distance quoted is the 12-coordinate distance.

^c For metals which exhibit more than one phase the table indicates the phase for which data have been taken. Manganese exhibits a large number of phases, none of which has an idealised structure.

Table 2

Bond length and bond enthalpy data for metals and metal carbonyls, including calculated metal–ligand bond enthalpies^a

	Experimental $\Delta H_{\text{disrupt}}$ (kJ mol ⁻¹)	$d(\text{M–M})$ (pm)	$E(\text{M–M})$ (kJ mol ⁻¹)	$\Sigma E(\text{M–M})$ (kJ mol ⁻¹)	$E(\text{M–CO})$ (kJ mol ⁻¹)
Fe	417(4)	248	75		–
Fe(CO) ₅	585(8)	–	–	0	117
Fe ₂ (CO) ₉	1173(25)	252	70	70	123
Fe ₃ (CO) ₁₂	1676(29)	256 and 268 (2 off)	65 and 52	169	126
Ru	651(8)	265	109		
Ru ₃ (CO) ₁₂	2414(29)	285	78	234	182
Os	790(8)	268	132		
Os ₃ (CO) ₁₂	2690(29)	288	94	282	201
Co	428(2)	251	71		
Co ₂ (CO) ₈	1160(12)	252	70	70	136
Co ₄ (CO) ₁₂	2121(29)	249	74	444	140
Rh	557	269	93		
Rh ₄ (CO) ₁₂	2648(29)	273	86	516	178
Rh ₆ (CO) ₁₆	3874(29)	278	80	960	182
Ir	665(8)	271	111		
Ir ₄ (CO) ₁₂	3051(29)	268	117	702	196

^a Data are taken from Ref. [22].



The clusters $\text{Fe}_2(\text{CO})_9$, $\text{M}_3(\text{CO})_{12}$ ($\text{M} = \text{Fe}$, Ru and Os), $\text{Co}_2(\text{CO})_8$, $\text{M}'_4(\text{CO})_{12}$ ($\text{M}' = \text{Co}$, Rh and Ir) and $\text{Rh}_6(\text{CO})_{16}$ had all been structurally characterised and found to contain metal–metal bonds of length very similar to those to nearest neighbour atoms in the bulk metal (generally, but not exclusively, longer than those in the bulk metal). Using the appropriate relationship $E = A d^{-4.6}$ for the metal in question to deduce the strength of the individual metal–metal bonds in these clusters, it was possible to calculate the value of $\Sigma E(\text{M-M})$ and express this as a percentage, $100 \Sigma E(\text{M-M})/\Delta H_{\text{dis}}$, of the disruption enthalpy. It was also possible to determine the average value of the metal–ligand bond enthalpy terms, $E(\text{M-CO})$, in these clusters, computed as $[\Delta H_{\text{dis}} - \Sigma E(\text{M-M})]/y$. This treatment required no assumptions to be made about the numbers of electrons formally available for metal–metal bonding in these clusters, but simply assumed that the relationship between bond length and enthalpy held throughout, suggesting that the cluster bonds had enthalpies differing from those in the bulk metal by a few kJ mol^{-1} , though by as much as $30\text{--}40 \text{ kJ mol}^{-1}$ in cases like $\text{Ru}_3(\text{CO})_{12}$ and $\text{Os}_3(\text{CO})_{12}$. One feature stood out from the data in Table 2, in all of the cases for which metal–ligand bond enthalpies could be calculated for derivatives $\text{M}_x(\text{CO})_y$ of a particular metal of more than one nuclearity x ; the average value of $E(\text{M-CO})$ *increased* slightly as the nuclearity, x , increased, i.e. as the ratio of ligand molecules to metal atoms, y/x , *decreased*. This change in the apparent strength of binding of the ligand molecules, *increasing* as the competition with other ligands for available metal orbitals or electrons *decreases*, makes good chemical sense and suggests that the apportionment of bond enthalpies between the metal–metal and metal–ligand bonding in Table 2 is realistic. One would not need to increase $\Sigma E(\text{M-M})$ for the higher nuclearity clusters by much to cancel out or even reverse the trend in $E(\text{M-CO})$ with nuclearity. Indeed our calculated values of $\Sigma E(\text{M-M})$ may be slight overestimates for higher nuclearity clusters, as greater changes in $E(\text{M-CO})$ with nuclearity might have been expected. However, one should not overlook the capacity of carbonyl ligands to accommodate changes in the capacity of metal atoms for back- π -bonding that has already been alluded to. We believe that carbonyl ligands can bond to one or more metal atoms with a strength that is less affected by ligand:metal ratios than might initially be expected, because extra metal \rightarrow ligand back π -bonding, though strengthening the metal–ligand M-C bonds, weakens the ligand C-O bond, and the bond enthalpy term $E(\text{M-CO})$ will increase only to the extent that $E(\text{M-C})$ bond strengthening exceeds $E(\text{C-O})$ bond weakening.

A further reassuring feature of the data in Table 2 is that the values of $E(\text{M-CO})$ for the cluster species are fully in line with the values of $E(\text{M-CO})$ for mononuclear species such as $\text{Fe}(\text{CO})_5$ or other $\text{M}(\text{CO})_y\text{L}_z$ complexes [24] studied in which there is no metal–metal bonding to complicate the thermochemical analysis.

From Table 2, we are encouraged to conclude that $\Sigma E(\text{M-M})$ contributes only a small percentage of the total bond enthalpy, $\Sigma E(\text{M-M}) + \Sigma E(\text{M-CO})$, for these systems, some 6% for dinuclear clusters, 10% for trinuclear clusters, and 20–25% for tetranuclear and hexanuclear clusters.

The data in Table 2 are also in line with known enthalpies of adsorption of carbon monoxide to metal surfaces, and the significantly greater strength of metal–ligand than metal–metal bonds is consistent with experimental findings that exposure of metal surfaces to ligand vapours (e.g. H_2 , CO) can cause substantial structural realignment of the surface metal atoms [25], an effect of considerable importance for heterogeneous catalysis.

4. Neutral osmium clusters, $\text{Os}_x(\text{CO})_y$

In the previous section we showed that metal–metal bond enthalpies $E(\text{M–M})$ calculated for metal carbonyls of known heats of formation from bond lengths $d(\text{M–M})$ using relationships of the form $E = A d^{-k}$ provided realistic estimates of the total metal–metal bond enthalpies for these systems in that they led to estimates of average metal–ligand bond enthalpies of the expected magnitude, and that varied in an intelligible manner with cluster nuclearity. Here, we extend our discussion to some neutral carbonyl clusters formed by osmium that have been characterised structurally though not thermochemically [26]. Osmium is the metal probably most thoroughly characterised in its carbonyl cluster chemistry, thanks particularly to the synthetic and structural work of Johnson, Lewis, McPartlin, Raithby, Einstein, Pomeroy and their groups.

The known neutral osmium carbonyl clusters, $\text{Os}_x(\text{CO})_y$, that have been structurally characterised fall into three formula categories:

1. two compounds, $\text{Os}_3(\text{CO})_{12}$ and $\text{Os}_4(\text{CO})_{16}$, have a ligand:metal ratio y/x of 4:1, and are cyclic oligomers of $\text{Os}(\text{CO})_4$ units;
2. two other compounds, $\text{Os}_6(\text{CO})_{18}$ and $\text{Os}_7(\text{CO})_{21}$, have a ligand:metal ratio y/x of 3:1, and are compact aggregates (capped *closo* systems in PSEPT (polyhedron skeletal electron pair theory) terminology) of $\text{Os}(\text{CO})_3$ units;
3. five further clusters, with formulae $\text{Os}_4(\text{CO})_{14}$, $\text{Os}_4(\text{CO})_{15}$, $\text{Os}_5(\text{CO})_{16}$, $\text{Os}_5(\text{CO})_{18}$ and $\text{Os}_5(\text{CO})_{19}$ have ligand:metal ratios between 3 and 4, and contain both $\text{Os}(\text{CO})_3$ and $\text{Os}(\text{CO})_4$ units in arrays that are intermediate in compactness between the open cyclic structures of $[\text{Os}(\text{CO})_4]_3$ or 4 and the capped-*closo* structures of $[\text{Os}(\text{CO})_3]_6$ or 7.

The structures of these clusters are illustrated in Fig. 3, which shows that, like metal carbonyl clusters $\text{M}_x(\text{CO})_y$ in general, these compounds have structures that, for a given nuclearity, x , become progressively more open, with fewer points of bonding contact between their metal atoms, as the ligand:metal ratio y/x increases. Not only do the numbers of their metal–metal bonds decrease, but their remaining individual metal–metal bonds get progressively longer on average as y/x increases. This is a familiar feature of cluster structural chemistry. In PSEPT terminology, when n skeletal atoms are held together by $(n + 1)$ skeletal electron pairs, compact *closo* n -vertex deltahedral structures are found. Systems with fewer skeletal electron pairs adopt capped-*closo* (even more compact) structures like those of $\text{Os}_6(\text{CO})_{18}$ and $\text{Os}_7(\text{CO})_{21}$. Systems with more skeletal electron pairs adopt more open (*nido*, *arachno* or *hypho*) structures, notionally fragments of progressively larger deltahedra.

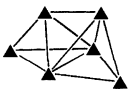
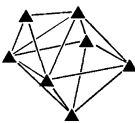
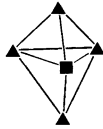


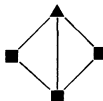
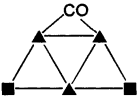
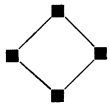
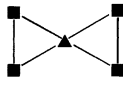
	6 pairs	7 pairs	8 pairs	9 pairs
mono-capped <i>closo</i>	 $\text{Os}_6(\text{CO})_{18}$	 $\text{Os}_7(\text{CO})_{21}$		
<i>closo</i>	 $\text{Os}_5(\text{CO})_{16}$			
<i>nido</i>	 $\text{Os}_4(\text{CO})_{14}$			
<i>arachno</i>	 $\text{Os}_3(\text{CO})_{12}$	 $\text{Os}_4(\text{CO})_{15}$	 $\text{Os}_5(\text{CO})_{18}$	
<i>hypho</i>			 $\text{Os}_4(\text{CO})_{16}$	 $\text{Os}_5(\text{CO})_{19}$

Fig. 3. Illustration of the structures of the neutral binary osmium carbonyls discussed in this work. The symbols \blacktriangle and \blacksquare are used to indicate the $\text{Os}(\text{CO})_3$ and $\text{Os}(\text{CO})_4$ vertices, respectively; bridging carbonyl ligands are drawn explicitly. The clusters are arranged according to their number of skeletal electron pairs and cluster class (PSEPT).

Of more interest to us here than the question of the shapes of osmium carbonyl clusters is the total enthalpy of their metal–metal bonds, $\Sigma E(\text{M}–\text{M})$. From the known structure of osmium (hcp, $d(\text{Os}–\text{Os})$ 267.54 pm) and enthalpy of atomisation (790.7 kJ mol^{−1}) we derive the expression $E(\text{Os}–\text{Os}) = 1.928 \times 10^{13} [d(\text{Os}–\text{Os})]^{-4.6}$ (for d in pm and E in kJ mol^{−1}). Using this to calculate bond enthalpy terms $E(\text{Os}–\text{Os})$ for the individual bonds in osmium carbonyl clusters, and summing these to obtain $\Sigma E(\text{Os}–\text{Os})$ for each of the nine compounds $\text{Os}_x(\text{CO})_y$ mentioned above, and dividing the result by the cluster nuclearity, x , to obtain the total bond enthalpy per metal atom, $\Sigma E(\text{Os}–\text{Os})/x$, we find that the results fall on a smooth curve when plotted against y/x , Fig. 4. The curve necessarily passes through $\Sigma E(\text{Os}–\text{Os})/x = 0$ when $y/x = 5$, as $\text{Os}(\text{CO})_5$ is the formula of the mononuclear species and this complex has no metal–metal bonding. Moreover, the curve

can in principle be extrapolated to a value of $\Sigma E(\text{Os–Os})/x = 790.7 \text{ kJ mol}^{-1}$, the enthalpy of vaporisation of bulk osmium metal, when $y/x = 0$. Only the range from $y/x = 3$ to $y/x = 4$ can be covered by the values of $\Sigma E(\text{Os–Os})/x$ we have calculated for known neutral osmium carbonyls, since the known compounds all fall in this range, but we predict that any new osmium carbonyl clusters prepared and structurally characterised in future will have structures for which calculated values of $\Sigma E(\text{Os–Os})/x$ will fall on or near the same smooth curve, whether y/x lies between 3 and 4 or outside those limits.

Slightly differing values of $\Sigma E(\text{Os–Os})/x$ are obtained for the pairs of compounds with identical y/x ratio (3.0 or 4.0). These slight differences reflect the efficiencies with which these oligomers $[\text{Os}(\text{CO})_3]_x$ and $[\text{Os}(\text{CO})_4]_x$ form their metal–metal bonds, possibly impeded slightly by non-bonded repulsions between their carbonyl ligands; the 12 carbonyl ligands in the triangular cluster $\text{Os}_3(\text{CO})_{12}$ appear to be less crowded than the 16 carbonyl groups in the flattened butterfly-shaped cluster $\text{Os}_4(\text{CO})_{16}$, so accounting for the small difference between the values of $\Sigma E(\text{Os–Os})/x$ for these species (94 and 87 kJ mol^{-1} , respectively). The (weak) metal–metal bonds in the tetranuclear cluster $\text{Os}_4(\text{CO})_{16}$ have apparently stretched relative to those in the trinuclear $\text{Os}_3(\text{CO})_{12}$ to allow efficient bonding to the larger total number of carbonyl ligands accommodated. Although $\text{Os}_6(\text{CO})_{18}$ and $\text{Os}_7(\text{CO})_{21}$ have even more ligand molecules to accommodate, these are grouped around significantly larger (higher nuclearity) metal aggregates, and so do not differ significantly in the efficiency with which they form metal–metal bonds ($\Sigma E(\text{Os–Os})/x$ values of 215 and 218 kJ mol^{-1} , respectively).

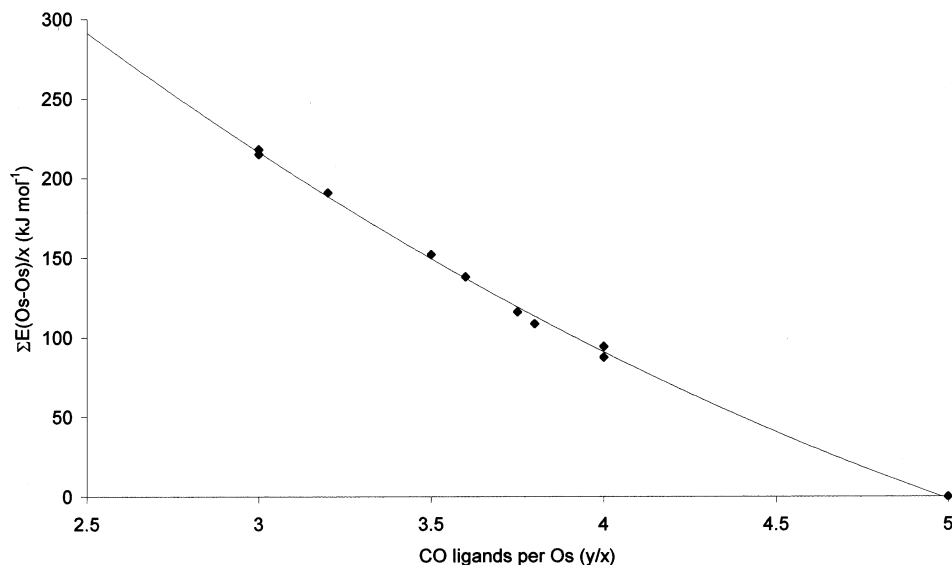


Fig. 4. The relationship between the total metal–metal bond enthalpy per metal atom, $\Sigma E(\text{Os–Os})/x$, in $\text{Os}_x(\text{CO})_y$ clusters and the number of carbonyl ligands per metal atom (y/x).

Table 3

The known structurally characterised binary osmium carbonyl clusters $[\text{Os}_x(\text{CO})_y]$ listing $\Sigma E(\text{Os-Os})$, $\Sigma E(\text{M-CO})$, ΔH_{dis} of $\text{Os}_x(\text{CO})_y(\text{g})$ to $\text{Os}(\text{g})$ and $\text{CO}(\text{g})$ and $\Delta_f H$ of $\text{Os}_x(\text{CO})_y(\text{g})$

Cluster	$\Sigma E(\text{Os-Os})$ (kJ mol ⁻¹)	$\Sigma E(\text{Os-CO})$ (kJ mol ⁻¹)	ΔH_{dis} (kJ mol ⁻¹)	$\Delta_f H$ (kJ mol ⁻¹)
$\text{Os}_3(\text{CO})_{12}$	283	2412	2695	-1651
$\text{Os}_4(\text{CO})_{14}$	608	2862	3470	-1857
$\text{Os}_4(\text{CO})_{15}$	464	3039	3503	-2001
$\text{Os}_4(\text{CO})_{16}$	349	3216	3565	-2173
$\text{Os}_5(\text{CO})_{16}$	955	3312	4267	-2085
$\text{Os}_5(\text{CO})_{18}$	690	3694	4384	-2423
$\text{Os}_5(\text{CO})_{19}$	543	3843	4386	-2536
$\text{Os}_6(\text{CO})_{18}$	1290	3762	5052	-2301
$\text{Os}_7(\text{CO})_{21}$	1526	4389	5915	-2706

Our capacity to extend this discussion to the strength of the metal–ligand bonds in these neutral osmium carbonyl clusters is limited by the fact that only one of them, $\text{Os}_3(\text{CO})_{12}$ [9], has been subjected to a calorimetric study, which afforded an enthalpy of formation, $\Delta_f H$ of -1651 ± 30 kJ mol⁻¹, and of disruption into gaseous metal atoms and carbon monoxide molecules, ΔH_{dis} of 2695 ± 30 kJ mol⁻¹. As $\Sigma E(\text{Os-Os})$ for this molecule was calculated to be 283 kJ mol⁻¹, $\Sigma E(\text{Os-CO})$ was inferred to be 2412 kJ mol⁻¹, and so the average metal–ligand bond enthalpy term, $E(\text{Os-CO})$, is 201 ± 3 kJ mol⁻¹. Clearly, further calorimetric studies on this and other osmium carbonyls are needed to corroborate this finding and shed further light on whether (and by how much) the metal–ligand bond enthalpy terms, $E(\text{Os-CO})$, vary with ligand:metal ratios in the manner evident from the data in Table 2 for other metal carbonyls. If they do, and using $E(\text{Os-CO}) = 201$ kJ mol⁻¹ as a reliable figure for $\text{Os}_3(\text{CO})_{12}$, we estimate that $E(\text{Os-CO})$ for each carbonyl ligand in the $\text{Os}(\text{CO})_3$ units of the species $\text{Os}_6(\text{CO})_{18}$ and $\text{Os}_7(\text{CO})_{21}$ should be ca. 209 kJ mol⁻¹ with intermediate values of $E(\text{Os-CO})$ for the mixed $\text{Os}(\text{CO})_3$ and $\text{Os}(\text{CO})_4$ fragments in other $\text{Os}_x(\text{CO})_y$ clusters. Estimates of the enthalpies of formation, $\Delta_f H^\circ$, of these osmium carbonyl clusters, $\text{Os}_x(\text{CO})_y$ made on this basis are given in Table 3.

Structural evidence of a variation in metal–ligand bond strengths as the ratio of ligand molecules to metal atoms is varied is already available in the form of the slight but apparently significant variations in the metal–carbon and carbon–oxygen distances with ligand:metal ratios, y/x , for osmium carbonyl clusters, $\text{Os}_x(\text{CO})_y$. In our introduction we remarked on the familiar π -acidity of carbonyl ligands that allows the strength of binding of carbon monoxide to a metal centre to be increased by electron transfer from filled metal d (or pd hybrid) orbitals into ligand CO π^* orbitals. Such back- π -bonding increases the multiplicity of the metal–carbon bond at the expense of a weakening of the C–O bond. An osmium atom bound to three carbonyl ligands is expected to be able to participate in more π -back bonding to each of these ligands than when bound to four carbonyl ligands, so is expected to

form slightly shorter Os–C bonds. In turn, the carbon–oxygen bond distances, $d(\text{C–O})$, in $\text{Os}(\text{CO})_3$ units in clusters are expected to be longer than those in $\text{Os}(\text{CO})_4$ units. The differences in bond lengths are, however, expected to be slight, and the precision with which individual bond lengths have been determined in the past have rarely been sufficient to reveal such effects unambiguously. The greater length and lower bond order of the metal–carbon bonds in carbonyl complexes should allow such effects to be seen more readily than in their carbon–oxygen bond distances, for which a change in bond length of only 1 pm corresponds to a bond enthalpy change of some 40 kJ mol^{-1} .

Figs. 5 and 6 show how the mean metal–carbon and carbon–oxygen bond distances in osmium carbonyl clusters, $\text{Os}_x(\text{CO})_y$, vary with the ligand:metal ratio y/x . The mean metal–carbon distances decrease by about 3 pm from ca. 193 to 190 pm as y/x is increased from 3 (as in $\text{Os}_6(\text{CO})_{18}$ and $\text{Os}_7(\text{CO})_{21}$) to 4 (as in $\text{Os}_3(\text{CO})_{12}$ and $\text{Os}_4(\text{CO})_{16}$). The mean carbon–oxygen distance increases over the same range of y/x values by just over 1 pm. Interpreting the published structural data is complicated by variations in the refinement methods that have been used from one compound to another. The carbon atom appears to ‘slide’ along the metal–oxygen vector as the refinement method is changed [27]. Isotropic refinement of all relevant carbon and oxygen atoms leads to shorter Os–C and longer C–O distances than are found when both carbon and oxygen atoms are refined anisotropically. For that reason, in Fig. 5, which shows how $d(\text{Os–C})$ varies with y/x , the data effectively fall on two parallel straight lines. The upper line, with data points shown as closed circles, represents $\text{Os}_3(\text{CO})_{12}$ (all atoms anisotropic) and $\text{Os}_5(\text{CO})_{19}$, $\text{Os}_4(\text{CO})_{14}$ and $\text{Os}_6(\text{CO})_{18}$, for all of which the metal and oxygen atoms were refined anisotropically and only the carbon atoms isotropically. The lower line, shown as open circles,

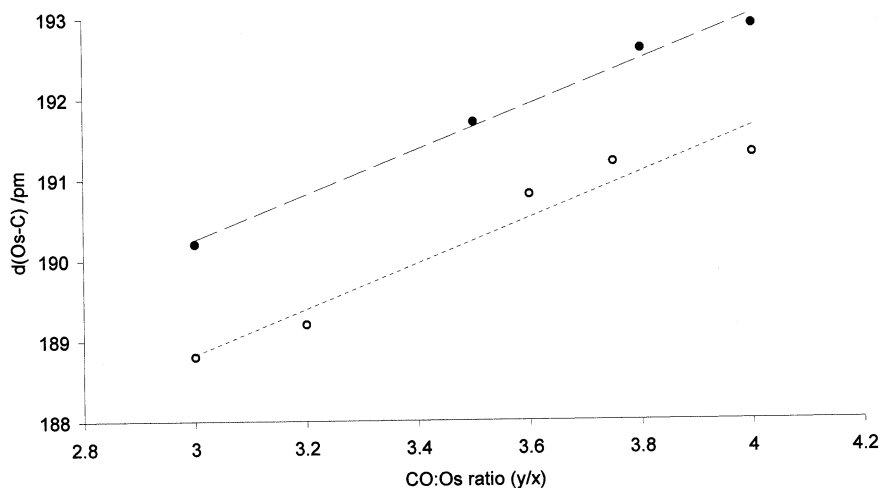


Fig. 5. Plot of $d(\text{Os–C})$ for osmium carbonyl clusters $\text{Os}_x(\text{CO})_y$ as a function of y/x (see text for details of the two sets of data).

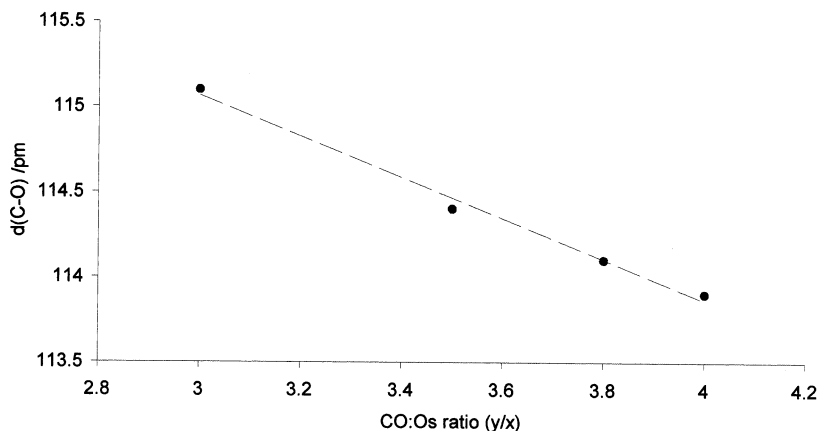


Fig. 6. Plot of $d(\text{CO})$ for osmium carbonyl clusters $\text{Os}_x(\text{CO})_y$, as a function of y/x (see text for details of the included data points).

represents structures for which only the metal atoms were refined anisotropically, whereas both carbon and oxygen were refined isotropically, generally because too few reflections were observed to allow refinement of more parameters. Only the (more reliable) former type are shown in Fig. 6.

As more accurate determinations of metal–carbon and carbon–oxygen distances in polynuclear metal carbonyl complexes become available in future, as structural determinations become more precise, it is to be hoped that such trends as are illustrated in Figs. 5 and 6 will be more accurately documented. It should then be possible to assign bond energy terms, $E(\text{M}–\text{C})$ and $E(\text{C}–\text{O})$, to the metal–carbon and carbon–oxygen bonds in metal carbonyl complexes such that the metal–ligand bond enthalpies, $E(\text{M}–\text{CO})$, discussed here can be represented in terms of the metal–carbon bond enthalpy in the complex offset by the carbon–oxygen bond energy regained as the carbonyl ligand is removed:

$$E(\text{M}–\text{CO}) = E(\text{M}–\text{C}) - [E(\text{C}–\text{O})_{\text{free}} - E(\text{C}–\text{O})_{\text{bound}}]$$

Here, $E(\text{C}–\text{O})_{\text{free}}$ is the bond enthalpy term for a free, gaseous carbon monoxide molecule ($1076.5 \pm 0.4 \text{ kJ mol}^{-1}$) and $E(\text{C}–\text{O})_{\text{bound}}$ is the lower bond enthalpy term attributable to the longer carbon–oxygen bond in the coordinated ligand. As more crystallographic data of sufficient accuracy become available, it will become increasingly possible to calculate metal–carbon bond enthalpies from a combination of structural and calorimetric data and ultimately from structural data alone.

Further potential sources of information about the strengths of the carbon–oxygen bonds in metal carbonyl complexes are their vibrational frequencies, $\nu(\text{C}–\text{O})$, in their infrared spectra [10]. However, the exercise of relating vibrational frequencies to bond lengths and strengths is rarely straightforward, as coupling patterns vary too markedly between the systems to allow comparison [28]. Comparisons within series of complexes where the symmetry is retained, as in mononuclear octahedral

systems $\text{MoL}_3(\text{CO})_3$ or in tetrahedral $\text{LM}(\text{CO})_3$ or $\text{L}_3\text{M}(\text{CO})$ systems show that the stretching frequencies $\nu(\text{C}-\text{O})$ vary with L in a manner that reflects the expected competition between the carbonyl ligands and other ligands L for metal valence shell electrons and orbitals [29].

One example is known to us of an attempt to partition the metal–ligand bond enthalpy between metal–carbon and carbon–oxygen components. This was a discussion of the dinuclear iron carbonyl $\text{Fe}_2(\text{CO})_9$, which has a D_{3h} structure $(\text{CO})_3\text{Fe}(\mu^2\text{-CO})_3\text{Fe}(\text{CO})_3$ with six terminal and three bridging ligands [30]. The carbon–oxygen bonds of the bridging ligands are longer, $d(\text{C}-\text{O}) = 117.6(5)$ pm, than those in the terminal ligands, $d(\text{C}-\text{O}) = 115.6(4)$ pm. The assumptions necessary in the treatment, and the limited precision of the data, restricted the outcome of that discussion to the conclusion that the carbonyl ligands were probably bound as strongly in the terminal sites as in the bridging ones. This finding is consistent with what has subsequently been found to be the characteristic behaviour of carbonyl ligands on metal surfaces as well as metal clusters, where their π -acidic nature allows them to bind equally effectively, whether bridging or terminal. There is in some cases so little thermodynamic preference for one mode of bonding that changes between terminal and bridging sites may occur as a consequence of the loading level of ligand molecules on metal surfaces, and ligand fluxionality about the surfaces of metal clusters necessarily requires easy access from one terminal site to another on an adjacent metal atom via a bridged intermediate, or alternatively migration from one bridging site to another via a terminal intermediate. Indeed, such versatility lends support to the view that metal carbonyl cluster compounds can be regarded as polyhedra of ligand molecules, kept essentially regular by non-bonded repulsions, within which metal polyhedra rock, librate or rotate relatively readily because they bond equally effectively, whether the ligands are over the edges, faces or vertices of the metal polyhedron [31]. With the neutral osmium carbonyl complexes considered here, there is, however, a clear preference for the ligands to occupy terminal rather than bridging sites. In this connection it is interesting to note that the iron carbonyl $\text{Fe}_2(\text{CO})_9$ alluded to above apparently has no osmium counterpart $\text{Os}_2(\text{CO})_9$, perhaps because one or more of the ligands therein would need to play a bridging role, as in $(\text{OC})_4\text{Os}(\mu^2\text{-CO})\text{Os}(\text{CO})_4$ or $(\text{OC})_3\text{Os}(\mu^2\text{-CO})_3\text{Os}(\text{CO})_3$. An unsymmetrical, polar unbridged structure $(\text{CO})_4\text{OsOs}(\text{CO})_5$ would be extremely unlikely, since it would be expected to be unstable with respect to $\text{Os}(\text{CO})_5$ and $[\text{Os}(\text{CO})_4]_n$. If $\text{Os}_2(\text{CO})_9$ were preparable, reference to Fig. 4 suggests that it would be expected to contain a metal–metal bond of enthalpy 81 kJ mol^{-1} and length 297 pm. Predictions about other osmium carbonyls yet to be prepared are to be found in Ref. [26].

5. Osmium carbonyl anions $[\text{Os}_x(\text{CO})_y]^{2-}$ and hydrides $[\text{Os}_x(\text{CO})_y\text{H}_z]^{c-}$; further characteristics of osmium carbonyl clusters

Many anionic osmium carbonyl clusters $[\text{Os}_x(\text{CO})_y]^{2-}$ and neutral or anionic carbonyl hydrides $[\text{Os}_x(\text{CO})_y\text{H}_z]^{c-}$ are now known, and have been structurally

characterised, though such systems have not been subjected to calorimetric determination of their enthalpies of formation. Interpretation of data on anionic systems would anyway require counter-ions to be specified and accounted for, and electron affinities and lattice energies of their salts to be calculated. Hydride structures would require assumptions to be made about the strength of binding of their hydride ligands. To venture far into such speculative territory would be inappropriate here. However, focusing attention on their total metal–metal bond enthalpies, $\Sigma E(\text{Os–Os})$, affords useful insight into the way the metal–metal bonding in these systems, like that in the neutral binary carbonyls $\text{Os}_x(\text{CO})_y$, reflects the electronic contribution towards metal–metal bonding made by their anionic charges and hydride and carbonyl ligands. We show below that the overall strength of the metal–metal bonding in such clusters reflects clearly and systematically the numbers of electrons provided by anionic charges or ligands to the metal atoms' valence shell.

The relationship (Fig. 4) already noted between $\Sigma E(\text{Os–Os})/x$ and y/x for neutral osmium carbonyls $\text{Os}_x(\text{CO})_y$ is intelligible in that the more ligands a set of metal atoms needs to accommodate, the more metal orbitals are required for metal–ligand bonding, and so the fewer are available for metal–metal bonding. Ligands in general vary in the number of electrons they contribute towards metal–ligand bonding, and so in the metal orbital demands they make. For anionic systems $[\text{Os}_x(\text{CO})_y]^{2-}$ or neutral or anionic carbonyl hydrides $[\text{Os}_x(\text{CO})_y\text{H}_z]^{c-}$, the overall strength of the metal–metal bonding is expected to reflect the numbers of electrons provided by the ligands and anionic charges, rather than just the numbers of

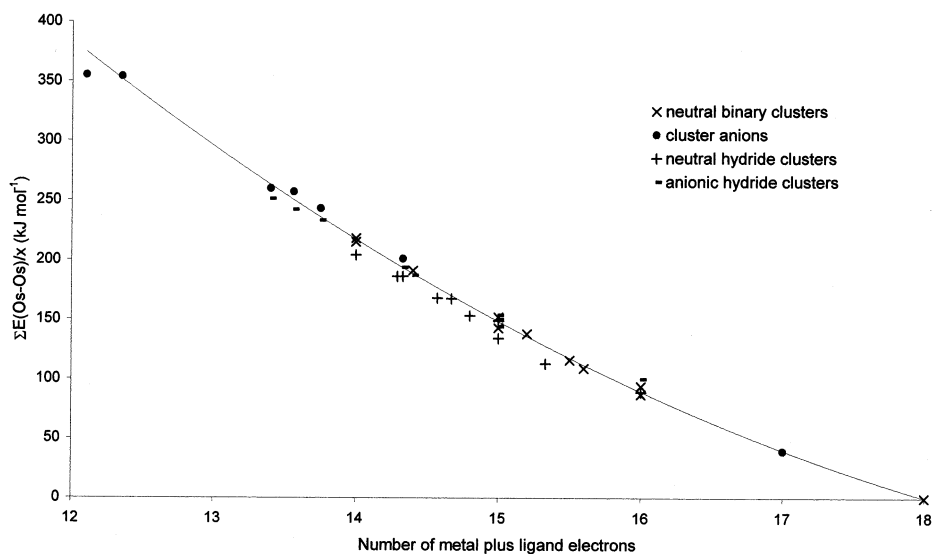


Fig. 7. Plot of total metal–metal bond enthalpy per osmium atom, $\Sigma E(\text{Os–Os})/x$, against the number of metal plus ligand electrons per osmium atom for four different classes of osmium carbonyl clusters.


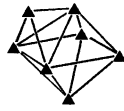
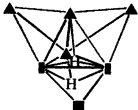




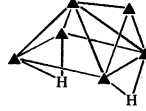

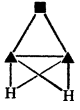
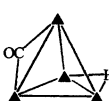
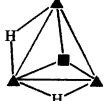
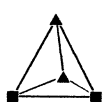


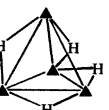
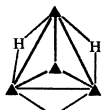
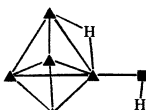
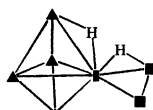
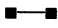
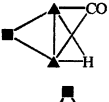
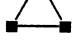
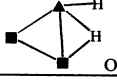
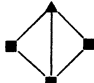
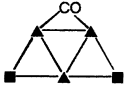
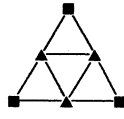


	5 pairs	6 pairs	7 pairs	8 pairs	9 pairs
<i>mono-capped closo</i>		 $\text{Os}_6(\text{CO})_{18}$	 $\text{Os}_7(\text{CO})_{21}$  $\text{Os}_7\text{H}_2(\text{CO})_{20}$		
<i>closo</i>		 $\text{Os}_5(\text{CO})_{16}$  $[\text{Os}_5\text{H}(\text{CO})_{15}]^-$	 $[\text{Os}_6(\text{CO})_{18}]^{2-}$  $[\text{Os}_6\text{H}(\text{CO})_{18}]^-$  $\text{Os}_6\text{H}_2(\text{CO})_{18}$	 $\text{Os}_7\text{H}_2(\text{CO})_{21}$	
<i>nido</i>	 $\text{Os}_3\text{H}_2(\text{CO})_{10}$	 $[\text{Os}_4\text{H}(\text{CO})_{13}]^-$  $\text{Os}_4\text{H}_2(\text{CO})_{13}$  $\text{Os}_4(\text{CO})_{14}$  $[\text{Os}_4\text{H}_2(\text{CO})_{12}]^{2-}$  $[\text{Os}_4\text{H}_3(\text{CO})_{12}]^-$  $\text{Os}_4\text{H}_4(\text{CO})_{12}$	 $\text{Os}_5\text{H}_2(\text{CO})_{16}$	 $\text{Os}_6\text{H}_2(\text{CO})_{19}$	 $\text{Os}_7(\text{CO})_{22}\text{H}_2$
<i>arachno</i>	 $[\text{Os}_2(\text{CO})_8]^{2-}$	 $[\text{Os}_3\text{H}(\text{CO})_{11}]^-$  $\text{Os}_3(\text{CO})_{12}$  $\text{Os}_3\text{H}_2(\text{CO})_{11}$	 $\text{Os}_4(\text{CO})_{15}$	 $\text{Os}_5(\text{CO})_{18}$	 $\text{Os}_6(\text{CO})_{17}[\text{P}(\text{OMe})_3]_4$
<i>hypho</i>		$[\text{Os}_2(\text{CO})_{10}]$		 $\text{Os}_4(\text{CO})_{16}$	 $\text{Os}_5(\text{CO})_{19}$

Fig. 8.

carbonyl ligands per metal atom. Accordingly, in Fig. 7, we plot $\Sigma E(\text{Os–Os})/x$ for these species, calculated as usual from the metal–metal bond lengths using the relationship $E(\text{Os–Os}) = 1.929 \times 10^{13} [d(\text{Os–Os})]^{-4.6}$, against the total number of electrons available per metal atom, expressed as metal valence shell electrons plus ligand electrons plus anionic charge electrons per metal atom, $(vx + 2y + z + c)/x$ for species $[\text{Os}_x(\text{CO})_y\text{H}_z]^c-$ (v , the number of valence shell electrons; $v = 8$ for osmium). Plotted thus, the limit, corresponding to $\text{Os}(\text{CO})_5$ or isoelectronic mononuclear species, has 18 electrons per metal atom. As expected, the data in Fig. 7 fall on essentially the same smooth curve as that in Fig. 4, showing that, whether electrons are provided by a carbonyl ligand, anionic charge or a hydride ligand, it is their *total electron number* that is important; the more ligand electrons per metal atom the system needs to accommodate, the less metal–metal bonding is possible.

Interestingly, the points in Fig. 7 show no systematic variation with the source of the extra electrons. It might have been expected that the values of $\Sigma E(\text{Os–Os})/x$ for anions $[\text{Os}_x(\text{CO})_y]^{2-}$ would be consistently higher than those for neutral carbonyl clusters, because their extra (anionic) electrons were not shared with ligand nuclei (as are the lone pair electrons formally donated by carbonyl ligands to form the ligand \rightarrow metal dative σ -bonds). There is just a hint of the opposite of such an effect in the cluster of data points in Fig. 7 relating to anions containing fewer than 14 metal plus ligand electrons per metal atom, though this cannot be regarded as significant. However, one effect worth noting is that of protonation of an anionic cluster $[\text{Os}_x(\text{CO})_y\text{H}_z]^c-$ to generate a species $[\text{Os}_x(\text{CO})_y\text{H}_{z+1}]^{(c-1)-}$. Although this does not change the total number of electrons within the cluster, it does modify the metal–metal bonding if the added proton plays a bridging role, $\text{Os}(\mu\text{-H})\text{Os}$, effectively converting a 2-centre 2-electron (2c2e) Os–Os bond into a (longer) 3-centre 2-electron (3c2e) Os–H–Os bond, and so lowering the (calculated) metal–metal bond enthalpy. Significantly, in Fig. 7, for clusters that contain the same number of electrons per metal atom, the neutral osmium carbonyl hydride clusters, $\text{Os}_x(\text{CO})_y\text{H}_z$ produce the data points with the lowest values of $\Sigma E(\text{Os–Os})/x$.

The slight curvature of the plots of $\Sigma E(\text{Os–Os})/x$ against y/x or $(8x + 2y + z + c)/x$ in Figs. 4 and 7, increasing in slope as the numbers of electrons per metal atom decrease, is worth noting. As more electrons become available for metal–metal (as opposed to metal–ligand) bonding, they are used more efficiently. The metal–metal bonds in small clusters are typically 10–15% longer than those in the bulk metals. Those in larger clusters are closer in length to those in the bulk metal. This is consistent with the idea that the bonding in clusters becomes more ‘metallic’ as cluster size increases, and that metal–ligand bonding effects become progressively more dominant as cluster sizes decrease.

Fig. 8. The geometries of the osmium carbonyls $[\text{Os}_x(\text{CO})_y]$, carbonyl anions $[\text{Os}_x(\text{CO})_y]^{2-}$, and neutral and anionic carbonyl hydrides $[\text{Os}_x(\text{CO})_y\text{H}_z]^c-$ with seven or fewer vertices, tabulated according to the cluster class and number of skeletal electron pairs. The symbols \blacktriangle and \blacksquare are used to indicate $\text{Os}(\text{CO})_3$ and $\text{Os}(\text{CO})_4$ vertices, respectively.

The shapes of the osmium clusters considered here are shown in Figs. 8 and 9 in which $\text{Os}(\text{CO})_4$ units are represented by filled squares, $\text{Os}(\text{CO})_3$ units by filled triangles, and metal–metal bonding contacts between them by straight lines. Hydride ligand sites (generally bridging) are shown where appropriate, as are the sites of those rare entities in osmium carbonyl cluster chemistry, bridging carbonyl groups, which significantly are found in relatively electron-rich, high carbonyl content systems such as $\text{Os}_5(\text{CO})_{18}$ or anionic systems such as $[\text{Os}_4\text{H}(\text{CO})_{13}]^-$ and $[\text{Os}_3\text{H}(\text{CO})_{11}]^-$, where the bridging carbonyl ligand withdraws electron density from the metal cluster more effectively than a terminal carbonyl ligand. For metal clusters in general, an overall negative charge appears to favour occupation of bridging sites by carbonyl ligands, so helping to spread the charge.

The osmium carbonyl clusters shown in Fig. 8 are displayed according to their PSEPT classification (*closo*, *nido*, etc.), which takes account of the number of electrons formally available for cluster bonding, assuming each metal atom uses three AOs for that purpose. Relatively compact deltahedral (*closo*) shapes are usual for n -atom clusters held together by $(n + 1)$ skeletal electron pairs. Yet more

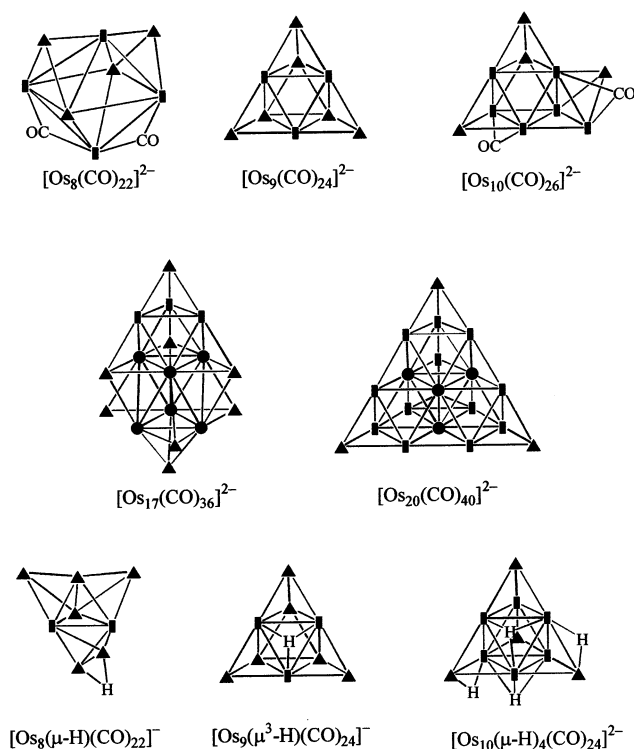


Fig. 9. The structures of the larger structurally characterised osmium carbonyl clusters. The following symbols are used: \blacksquare = $\text{Os}(\text{CO})_4$; \blacktriangle = $\text{Os}(\text{CO})_3$; \circ = $\text{Os}(\text{CO})_2$; \bullet = $\text{Os}(\text{CO})$. Hydride and bridging carbonyl ligands are drawn explicitly.

Table 4

The efficiency with which electron pairs are used in metal–metal bonding in some representative osmium carbonyl clusters $[\text{Os}_x(\text{CO})_y\text{H}_z]^{c-}$, expressed as metal–metal bond enthalpy $\Sigma E(\text{Os–Os})$ kJ mol^{−1} per skeletal electron pair, S_{ep} , and (in parentheses) per 2c2e metal–metal localized bond pair, S_{lb}

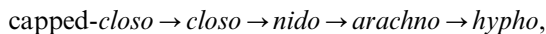
Cluster type	capped- <i>closo</i>	<i>closo</i>	<i>nido</i>	<i>arachno</i>	<i>hypho</i>
S_{ep} as function of x	x	$x + 1$	$x + 2$	$x + 3$	$x + 4$
			$\text{Os}_3\text{H}_2(\text{CO})_{10}$ 68 (85)	$\text{Os}_3\text{H}_2(\text{CO})_{11}$ 44 (89)	
			$\text{Os}_4(\text{CO})_{14}$ 101 (101)	$\text{Os}_4(\text{CO})_{15}$ 66 (93)	$\text{Os}_4(\text{CO})_{16}$ 44 (87)
		$\text{Os}_5(\text{CO})_{16}$ 159 (106)	$\text{Os}_5\text{H}_2(\text{CO})_{16}$ 109 (95)	$\text{Os}_5(\text{CO})_{18}$ 86 (99)	$\text{Os}_5(\text{CO})_{19}$ 60 (91)
	$\text{Os}_6(\text{CO})_{18}$ 215 (108)	$\text{Os}_6(\text{CO})_{18}^{2-}$ 172 (110)	$\text{Os}_6\text{H}_2(\text{CO})_{19}$ 126 (101)	$\text{Os}_6(\text{CO})_{17}\text{L}_4^{\text{a}}$ 96 (96)	
	$\text{Os}_7(\text{CO})_{21}$ 218 (109)	$\text{Os}_7\text{H}_2(\text{CO})_{21}$ 163 (100)	$\text{Os}_7\text{H}_2(\text{CO})_{22}$ 131 (98)		

^a L = P(OMe)₃.

compact (capped-*closo*) structures are normal for n -atom n -skeletal electron pair systems. Progressively more open (*nido*, *arachno*, *hypho*) shapes are found as the numbers of skeletal electrons increase to $(n + 2)$, $(n + 3)$ or $(n + 4)$ skeletal pairs, as the skeletal atoms can be thought of as occupying some of the vertices of the progressively larger polyhedra compatible with the numbers of electrons available.

A not uncommon misconception about PSEPT and related approaches to cluster shapes is that the skeletal electron pairs (S_{ep}) counted in such approaches (in order to identify the parent polyhedron on which the structure is regarded as based) are necessarily *bonding* electron pairs. This is true for *closo* and capped-*closo* species but progressively less so for *nido*, *arachno* or *hypho* species. The familiar cage opening that accompanies addition of more electron pairs to a particular number of skeletal atoms occurs because the extra electrons have to occupy orbitals that are metal–metal nonbonding or antibonding. (This is familiar at the ‘dinuclear cluster’ level in the progressive decrease in bond order in the sequence $\text{N}_2 > \text{O}_2 > \text{F}_2$ as the extra electrons associated with the two nuclei occupy progressively more π^* orbitals.)

A progressively decreasing return in terms of $\Sigma E(\text{Os–Os})/x$ is therefore expected for the electrons formally available for skeletal bonding as the cluster type changes in the sequence

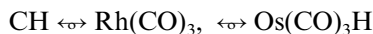


and the numbers of skeletal electron pairs available to the x metal atoms increase from x to $(x + 1)$, $(x + 2)$, $(x + 3)$ and $(x + 4)$. This is illustrated in Table 4, which lists the metal–metal bond enthalpy per skeletal electron pair, $E_{\text{sep}} = \Sigma E(\text{Os–Os})/S_{\text{ep}}$ for some representative osmium carbonyl species $[\text{Os}_x(\text{CO})_y\text{H}_z]^{c-}$. Although there is a general increase (with few exceptions) in the efficiency with which the

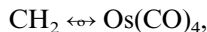
skeletal electron pairs formally available are used as cluster nuclearities increase (vertical columns in the table), the bond enthalpy return per skeletal electron pair, S_{ep} , decreases markedly as the structure type becomes more open (*closo* \rightarrow *nido* \rightarrow *arachno*, etc.; horizontal rows in the table).

An alternative method to PSEPT by which the skeletal bonding in cluster compounds can be rationalised, and that is particularly useful for small clusters, is in terms of 2c2e metal–metal bonds distributed in a manner consistent with the 18-electron rule. The difficulty with this approach is its incompatibility with some important categories of cluster compounds such as the large class of octahedral clusters, here exemplified by $\text{Os}_6(\text{CO})_{18}\text{H}_2$, containing 43 valence shell electron pairs. This is the right number of electrons for these to be regarded as *closo* 6-atom clusters held together by seven skeletal electron pairs, but one pair too many to allow each skeletal atom to participate in four skeletal bonds (not three, as in PSEPT), forming a 2c2e bond along an octahedral edge to each of its skeletal neighbours. Such clusters have to be regarded in localised bond terms as held together by 11 2c2e metal–metal bonds resonating around the 12 octahedral edges.

Despite these problems, the 2c2e localized bond approach still finds wide use, and it is instructive to explore whether our method of deriving metal–metal bond enthalpies is compatible with such an approach. If one divides the total metal–metal bond enthalpy, $\Sigma E(\text{Os–Os})$, computed using our length–enthalpy equation $E = 1.929 \times 10^{13} d^{-4.6}$, by the number (S_{lb}) of 2c2e localized bonds in the cluster compatible with the 18 electron rule, then one obtains values for a notional ‘single bond enthalpy’ for a 2c2e osmium–osmium bond, $E_{\text{lb}}(\text{Os–Os})$, that range from 87 to 109 kJ mol^{-1} for neutral carbonyls $\text{Os}_x(\text{CO})_y$, from 78 to 125 kJ mol^{-1} for anions $[\text{Os}_x(\text{CO})_y]^{2-}$, and from 85 to 102 kJ mol^{-1} for other species $[\text{Os}_x(\text{CO})_y\text{H}_z]^{e-}$. Values of E_{lb} for the species listed in Table 4 are shown in parentheses. The variations in E_{lb} from one system to another suggest that the once popular method of assigning ‘single bond’ enthalpies to such systems has serious limitations. The variations in E_{lb} , though less than those in E_{sep} , incidentally show similar trends, suggesting that electrons are used more effectively the higher the nuclearity and the more compact the structure, echoing the effects remarked on in connection with Figs. 4 and 7. Localized 2c2e metal–metal bond schemes are probably seen at their best in systems of low nuclearity ($x = 2, 3$ or 4) where similarities with organic systems stemming from isolobal relationships



and



allow ethane, cyclopropane, cyclobutane, or tetrahedrane analogues to be perceived in such metal carbonyls as $\text{Mn}_2(\text{CO})_{10}$, $\text{Os}_3(\text{CO})_{12}$, $\text{Os}_4(\text{CO})_{16}$ and $\text{Os}_4(\text{CO})_{12}\text{H}_4$.

Although in the absence of further thermochemical information on these systems $[\text{Os}_x(\text{CO})_y\text{H}_z]^{e-}$ it is difficult to comment on the relative stabilities of related systems arguing solely from structural data, further trends are evident than we have

already noted so far. The systems $[\text{Os}_x(\text{CO})_y\text{H}_z]^{c-}$ that have been structurally characterised include pairs of systems that, in formula type, differ by an $\text{Os}(\text{CO})_4$ unit, an $\text{Os}(\text{CO})_3$ unit, or an $\text{Os}(\text{CO})_2$ unit, though in this last case one of the pair has an $\text{Os}(\text{CO})_4$ unit where the other actually has two $\text{Os}(\text{CO})_3$ units. For example, formal addition of an $\text{Os}(\text{CO})_4$ unit, which has limited capacity for metal–metal bonding (it can provide one vacant orbital, or two electrons and two orbitals) raises $\Sigma E(\text{Os–Os})$ by 65–75 kJ mol^{-1} as shown by a comparison between $\text{Os}_3(\text{CO})_{12}$ ($\Sigma E = 283 \text{ kJ mol}^{-1}$) and $\text{Os}_4(\text{CO})_{16}$ ($\Sigma E = 349 \text{ kJ mol}^{-1}$). Formal addition of an $\text{Os}(\text{CO})_3$ unit, with a markedly greater capacity for metal–metal bond formation (two vacant orbitals, or three orbitals and two electrons) raises $\Sigma E(\text{Os–Os})$ by ca. 200–220 kJ mol^{-1} (cf. $\text{Os}_3(\text{CO})_{12}$, $\Sigma E = 283 \text{ kJ mol}^{-1}$, $\text{Os}_4(\text{CO})_{15}$, $\Sigma E = 464 \text{ kJ mol}^{-1}$, and $\text{Os}_5(\text{CO})_{18}$, $\Sigma E = 690 \text{ kJ mol}^{-1}$). An $\text{Os}(\text{CO})_2$ unit has a still greater capacity for metal–metal bonding (three vacant orbitals) and it is no surprise that pairs of systems formally differing by such a unit differ in $\Sigma E(\text{Os–Os})$ by some 320–330 kJ mol^{-1} (e.g. compare $\text{Os}_3(\text{CO})_{12}$, 283 kJ mol^{-1} and $\text{Os}_4(\text{CO})_{14}$, 608 kJ mol^{-1}).

Comparisons between systems of more direct relevance to their experimental behaviour can be made if one examines the effects of ligand loss or addition. For example, addition of an extra carbonyl ligand to a cluster, as in the conversion of $\text{Os}_4(\text{CO})_{14}$ into $\text{Os}_4(\text{CO})_{15}$, causes loss of ca. 128 kJ mol^{-1} in the metal–metal bond enthalpy. Such a reaction will be exothermic if $E(\text{M–CO})$ for the new metal–ligand bond formed in the process has the expected value of ca. 200 kJ mol^{-1} , though the thermodynamics will be influenced by entropic factors [32] that will partly offset such enthalpic considerations.

The tendency of osmium carbonyls to add dihydrogen can be examined by consideration of three pairs of compounds that differ by two hydride ligands (values of $\Sigma E(\text{Os–Os})$ in kJ mol^{-1} in parentheses);

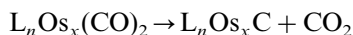
$\text{Os}_5(\text{CO})_{16}$ (955) and $\text{Os}_5(\text{CO})_{16}\text{H}_2$ (763),
 $\text{Os}_6(\text{CO})_{18}$ (1290) and $\text{Os}_6(\text{CO})_{18}\text{H}_2$ (1114);
 and $\text{Os}_7(\text{CO})_{21}$ (1526) and $\text{Os}_7(\text{CO})_{21}\text{H}_2$ (1300).

Experimental studies suggest that oxidative addition of dihydrogen to the metal carbonyl clusters is essentially a thermoneutral process in each of these three cases. From this, it has been deduced [33] that the metal–hydrogen bond enthalpies $E(\text{Os–H})$ in the carbonyl hydrides have values in the region of $306 \pm 25 \text{ kJ mol}^{-1}$. The actual sites occupied by hydrogen ligands in osmium carbonyl hydrides have rarely been established unambiguously by neutron diffraction studies, but have been inferred from gaps in the carbonyl ligand coordination sphere, or deduced from potential energy calculations [34], the preferred sites being over Os–Os polyhedron edges, edges that in localized bond terms can be thought of as bound by 3c2e Os–H–Os bridge bonds. The best estimates currently available [33] of the enthalpies of osmium–hydrogen bonds are $E(\text{Os–H}) = 264 \pm 10 \text{ kJ mol}^{-1}$ and $E(\text{Os–H–Os}) = 324 \pm 10 \text{ kJ mol}^{-1}$.

6. Osmium carbonyl carbide clusters, $[\text{Os}_x(\text{CO})_y\text{H}_x\text{C}]^{c-}$

One other category of osmium carbonyl cluster is known that is worth a brief introductory discussion here, though it has not, to our knowledge, been discussed previously in a thermochemical context. This is the category in which an interstitial carbon atom occupies a core position at the centre of the metal cluster, usually surrounded by an octahedral array of metal atoms. Such compounds are usually referred to as metal carbonyl cluster ‘carbides’, though the name, implying the presence of anionic C^{4-} , is misleading. Surrounded by six metal atoms in an octahedral array, such compounds are more appropriately regarded as carbocationic rather than anionic, though we shall reserve discussion of that until later when, in the cases of rhenium and rhodium clusters, there are more systems containing interstitial or core atoms to consider.

Osmium carbonyl clusters containing core carbon atoms usually result from the thermal decomposition of smaller clusters, when there is loss not only of carbon monoxide (leading to more compact, often highly capped *closo* structures containing a lower ligand:metal ratio y/x than in the original compound that has undergone thermal decomposition) but also loss of some carbon dioxide. The latter results from a disproportionation reaction between two carbonyl ligands that leads to a core carbon atom and expulsion of carbon dioxide:



(L_n represents the other ligands present that do not participate in the reaction). Known examples of osmium carbonyl carbides that have been formed in such reactions and have been structurally characterised include the anionic system [35] $[\text{Os}_{10}(\text{CO})_{24}\text{C}]^{2-}$ and its protonated variants $[\text{Os}_{10}(\text{CO})_{24}\text{HC}]^{-}$ and $[\text{Os}_{10}(\text{CO})_{24}\text{H}_2\text{C}]$ [36,37], which have tetra-capped octahedral structures in which the core carbon atom is at the octahedron centre, where all four of its valence shell electrons have to be reckoned as contributed to the skeletal electron count. These clusters are effectively isoelectronic with the species $[\text{Os}_{10}(\text{CO})_{26}]^{2-}$ and $[\text{Os}_{10}(\text{CO})_{24}\text{H}_4]^{2-}$ which contain no core carbon atoms. Having the same number of valence shell electrons per metal atom as the latter, the core carbon systems should have similar $\Sigma E(\text{Os}-\text{Os})$, and hence $\Sigma E(\text{Os}-\text{Os})/x$, values. The actual values for these five isoelectronic clusters are given in Table 5.

The difference between $[\text{Os}_{10}(\text{CO})_{26}]^{2-}$ and $[\text{Os}_{10}(\text{CO})_{24}\text{H}_4]^{2-}$ results from the bridging hydride effect already referred to, wherein conversion of Os–Os links into Os–H–Os links increases the metal–metal separation, reducing $\Sigma E(\text{Os}-\text{Os})$ but adding an $E(\text{Os}-\text{H}-\text{Os})$ term to the thermodynamic balance. It is interesting that, although roughly of the expected magnitude, the values of $\Sigma E(\text{Os}-\text{Os})/x$ for the core carbide systems are all a little lower than those of the analogous clusters containing no core carbon atoms. As the shapes of these systems are the expected tetra-capped octahedra (though $[\text{Os}_{10}(\text{CO})_{26}]^{2-}$, which has to accommodate two more carbonyl ligands at its surface, differs subtly in having the fourth capping atom capping one of the capping faces rather than one of the fundamental octahedral faces) the $\Sigma E(\text{Os}-\text{Os})$ values reflect the slightly longer metal–metal links

Table 5

The Os₁₀ clusters discussed, including those containing core carbon atoms, listing $\Sigma E(\text{Os–Os})$ for the Os₁₀ unit, and $\Sigma E(\text{Os–Os})$ separately calculated for the central Os₆ octahedron and the Os–Os bonds to the capping atoms

Cluster	$\Sigma E(\text{Os–Os})$ (kJ mol ^{−1})	$\Sigma E(\text{Os–Os})/x$ (kJ mol ^{−1})	$\Sigma E(\text{Os–Os})$ for Os ₆ (kJ mol ^{−1})	$\Sigma E(\text{Os–Os})$ for caps (kJ mol ^{−1})
[Os ₁₀ (CO) ₂₆] ^{2−}	2603	260.3	1307	1296
[Os ₁₀ (CO) ₂₄ H ₄] ^{2−}	2513	251.3	1231	1282
[Os ₁₀ (CO) ₂₄ C] ^{2−}	2490	249.0	1178	1312
[Os ₁₀ (CO) ₂₄ HC] [−]	2432	243.2	1169	1263
[Os ₁₀ (CO) ₂₄ H ₂ C]	2451	245.1	1191	1260

in the compounds containing the core carbon atoms, which presumably require a little more space than would have been provided had the octahedron edge lengths been in line with the expected values for such systems. Significantly, it is the Os–Os distances in the octahedral coordination sphere of the core carbon atoms in these systems that are longer than those in the clusters which do not contain core carbon atoms. This can be quantified by determining the bond enthalpies, $E(\text{Os–Os})$, associated with the Os₆ octahedra in these clusters (Table 5), which confirm that the largest contribution to the lower $\Sigma E(\text{Os–Os})$ values of the core-carbon containing clusters comes from longer, weaker bonds in the central Os₆ octahedron, there being far less variation in the contribution to $\Sigma E(\text{Os–Os})$ from the bonds to the capping atoms, although a detailed discussion of the data is complicated by the presence of varying numbers and locations of hydride ligands. We conclude that the effective radius of a core carbon atom in an octahedral osmium cluster is greater than that ($274 \times 0.414 \times 0.5 = 56.7$ pm) which is formally available in such a cluster as [Os₁₀(CO)₂₆]^{2−}, and so the core carbon atom shoulders the osmium atoms a little further apart. The effective radius of the core carbon atoms in these osmium clusters is approximately 60 pm ($290 \times 0.414 \times 0.5$), much less than the single bond covalent radius of carbon in familiar organic systems (77 pm). We shall return to a discussion of systems containing core carbon atoms later, in connection with rhenium, rhodium and binary metal carbides of early transition metals.

7. Rhenium carbonyl clusters, [Re_x(CO)_yH_z]^{c−} and [Re_x(CO)_yH_zC]^{c−}

Although less is known about rhenium carbonyl cluster chemistry than osmium carbonyl cluster chemistry, the number of rhenium carbonyl clusters, including carbonyl hydrides [Re_x(CO)_yH_z]^{c−} of nuclearities $x=2$ to 6 that have been structurally characterised totals about 20 (Fig. 10). In addition, several rhenium carbonyl carbides of general formulae [Re_x(CO)_yH_zC]^{c−} have been structurally characterised, the carbide carbon usually occupying a central octahedral site. Such systems not only offer scope to extend to rhenium the types of discussions already

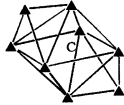

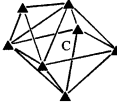
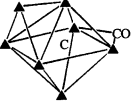
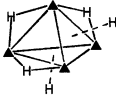
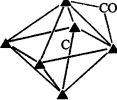
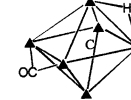
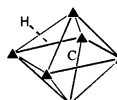
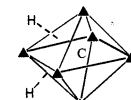
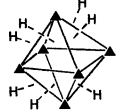
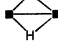
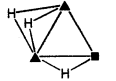
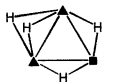


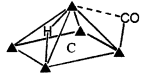
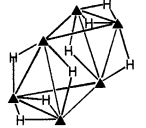
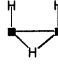
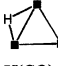
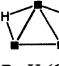
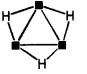


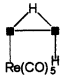
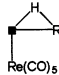
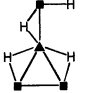
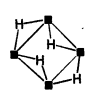
	4 pairs	5 pairs	6 pairs	7 pairs	8 pairs
<i>disapped closo</i>				 $[\text{Re}_8\text{C}(\text{CO})_{24}]^{2-}$	
<i>capped closo</i>	 $[\text{Re}_4\text{H}_4(\text{CO})_{12}]$			 $[\text{Re}_7\text{C}(\text{CO})_{21}]^{3-}$ $[\text{Re}_7\text{C}(\text{CO})_{21}\text{H}]^{2-}$ $[\text{Re}_7\text{C}(\text{CO})_{21}\text{H}_2]^{-}$  $[\text{Re}_7\text{C}(\text{CO})_{22}]^{-}$	
<i>closo</i>		 $[\text{Re}_4\text{H}_5(\text{CO})_{12}]^{-}$		 $[\text{Re}_6\text{C}(\text{CO})_{19}]^{2-}$  $[\text{Re}_6\text{C}(\text{CO})_{19}\text{H}]^{-}$  $[\text{Re}_6\text{C}(\text{CO})_{18}\text{H}]^{3-}$  $[\text{Re}_6\text{C}(\text{CO})_{18}\text{H}_2]^{2-}$  $[\text{Re}_6\text{H}_7(\text{CO})_{18}]^{-}$	
<i>nido</i>	 $[\text{Re}_2\text{H}_2(\text{CO})_8]$	 $[\text{Re}_3\text{H}_3(\text{CO})_{10}]^{2-}$  $[\text{Re}_3\text{H}_4(\text{CO})_{10}]^{-}$	 $[\text{Re}_4\text{H}_4(\text{CO})_{13}]^{2-}$  $[\text{Re}_4\text{H}_6(\text{CO})_{12}]^{2-}$	 $[\text{Re}_5\text{C}(\text{CO})_{16}\text{H}]^{2-}$	 $[\text{Re}_6\text{H}_8(\text{CO})_{18}]^{2-}$
<i>arachno</i>		 $[\text{Re}_2\text{H}_2(\text{CO})_8]^{-}$ $(\text{OC})_5\text{Re}$ $[\text{Re}_2(\text{CO})_{10}]$	 $[\text{Re}_3\text{H}(\text{CO})_{12}]^{2-}$  $\text{Re}_3\text{H}_2(\text{CO})_{12}]^{-}$  $[\text{Re}_3\text{H}_3(\text{CO})_{12}]$	 $[\text{Re}_4(\text{CO})_{16}]^{2-}$  $[\text{Re}_4\text{H}_5(\text{CO})_{14}]^{-}$	
<i>hypho</i>				 $[\text{Re}_3\text{H}_2(\text{CO})_{13}]^{-}$  $[\text{Re}_3\text{H}(\text{CO})_{14}]$	 $[\text{Re}_4\text{H}_4(\text{CO})_{15}]^{2-}$  $[\text{Re}_4\text{H}_4(\text{CO})_{16}]$

Fig. 10.

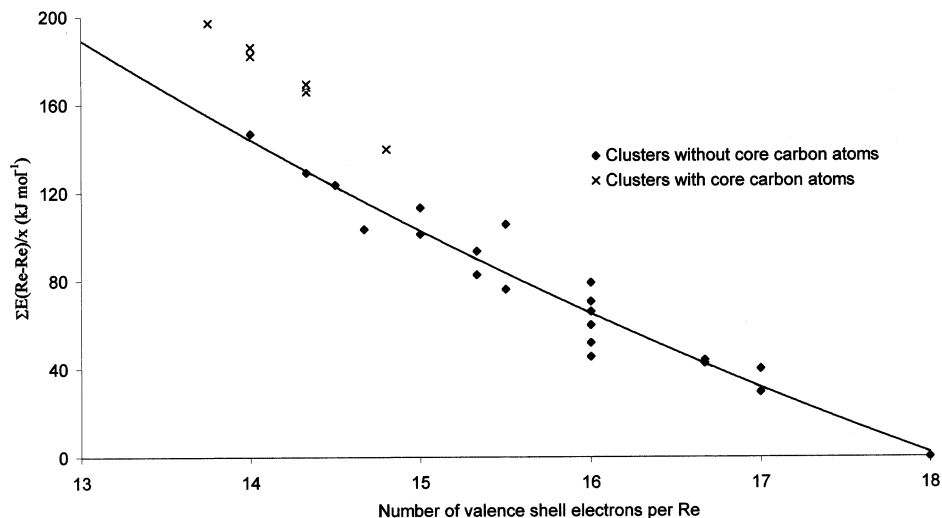


Fig. 11. Plot of total metal–metal bond enthalpy per rhenium atom, $\Sigma E(\text{Re-Re})/x$, as a function of the number of valence shell electrons per metal atom for rhenium carbonyl clusters, both with and without core carbon atoms.

applied to osmium, but also allow the effect of core carbon atoms on cluster structures to be explored more fully than was possible with osmium.

Despite this wealth of structural information, little is known about the thermochemistry of rhenium carbonyl clusters, only one, $\text{Re}_2(\text{CO})_{10}$, having been subjected to calorimetric determination of its enthalpy of formation [9]. The known enthalpy of vaporisation of metallic rhenium (770 kJ mol^{-1}) and bond distance of 274.1 pm in its hexagonal close packed lattice lead to the equation

$$E(\text{Re-Re}) = 2.188 \times 10^{13} d^{-4.6}$$

for the metal–metal bond enthalpies we have calculated for all the rhenium carbonyl cluster systems known to us to have been structurally characterised [38]. The bond enthalpy data for rhenium clusters are listed in Ref. [38] and in Fig. 11 we plot $\Sigma E(\text{Re-Re})/x$ against the total number of electrons available per metal atom, $(7x + 2y + z + c + i)/x$, where x , y , z and c have their usual values and i , the number of electrons supplied by the interstitial atom, is 4 in the case of carbon.

As was the case with osmium, so with rhenium the metal–metal bond enthalpies per metal atom fall on or near a smooth curve that links the value for the bulk metal (770 kJ mol^{-1}) to a value of zero for 18-electron systems exemplified by $\text{Re}(\text{CO})_5\text{H}$ or $[\text{Re}(\text{CO})_5]^-$, though the scatter about that curve is greater than for osmium. Significantly, the points corresponding to clusters containing core carbon atoms, for which the carbon atom has been assumed throughout to supply four

Fig. 10. The geometries of the rhenium carbonyls $[\text{Re}_x(\text{CO})_y\text{H}_z]^{c-}$, and core carbon containing rhenium carbonyl clusters $[\text{Re}_x(\text{CO})_y\text{H}_z\text{C}]^{c-}$, tabulated according to the cluster class and number of skeletal electron pairs. The symbols \blacktriangle and \blacksquare are used to indicate $\text{Re}(\text{CO})_3$ and $\text{Re}(\text{CO})_4$ vertices, respectively.

electrons towards the skeletal electron count, fall on a different curve, with values of $\Sigma E(\text{Re-Re})/x$ exceeding those expected from the electron count (and found for species $[\text{Re}_x(\text{CO})_y\text{H}_z]^{c-}$ containing no core atom) by ca. 30 kJ mol⁻¹. These carbide values are some 25% higher than those expected.

One explanation for this effect — that the core carbon atoms are providing no electrons to the skeletal electron count, rather than the four electrons assumed — can be discounted. The core carbon atoms are at a distance from their neighbouring metal atoms that is clearly bonding. Indeed, the mean rhenium–rhenium distance in the octahedral hexanuclear cluster anion $[\text{Re}_6(\text{CO})_{19}\text{C}]^{2-}$ is 300.6 pm, implying a rhenium atom radius, at least in a metal–metal bonding direction of 150.3 pm. The implied maximum radius for the core carbon atom is $150.3 \times 0.414 = 62$ pm, significantly less than the single bond radius of carbon (77 pm). As indicated in our discussion of osmium clusters containing core carbon atoms, the term ‘carbide’ applied to such species is misleading in seeming to imply carbanion character, tending towards C^{4-} . In fact, the octahedrally coordinated carbon atoms are more closely related to the carbocationic environment exemplified in extreme form by the octahedral dicationic $[\text{C}(\text{AuPPh}_3)_6]^{2+}$ which itself may be regarded as a derivative of that elusive species, diprotonated methane, CH_6^{2+} , in which all of the one-electron hydrogen ligands of the latter are replaced by six one-electron AuPPh_3 ligands [39].

Such a carbocationic view of the environment provided for the core carbon atoms of metal carbonyl ‘carbide’ clusters is supported by ¹³C NMR studies. The ¹³C chemical shifts of a number of core-carbon metal clusters have been shown to relate to the effective radii of the carbon atoms, and interpreted in terms of a compression of (cationic) interstitial carbon atoms [40], though DFT calculations have offered a different interpretation of the NMR data [41]. Our view is that the data plotted in Fig. 11 support a model in which an incipiently cationic carbon atom, $\text{C}^{\delta+}$, of radius ≤ 62 pm, is pulling the metal atoms towards itself, leading to closer proximity of the metal atoms to each other than would be the case if there were no core atom, or if they were surrounding a significantly larger carbanion, and so generating a higher value of $\Sigma E(\text{Re-Re})$ than might have been expected from the electron count.

However, another factor is operating that should not be ignored. Reference to Fig. 10 will show that most known rhenium carbonyl clusters that do not contain core carbon atoms do, however, contain bridging hydride ligands, which as explained above tend to cause extension of the metal–metal bonds they bridge (in localized bond terms, effectively converting 2c2e MM bonds into 3c2e MHM bonds). So the metal–metal bond enthalpies for systems containing no interstitial carbon atoms but some Re–H–Re bridges will necessarily be lower than the values expected if no bridging hydrogen atoms were present. Though this bridging hydride effect must account for some of the enthalpy difference between the carbonyl hydride points on Fig. 11 and those relating to systems containing core carbon, it seems likely that the ‘normal’ curve should lie between these two extremes, as plotted.

Five datapoints in Fig. 11 relate to rhenium carbonyl clusters that contain 16 valence shell electrons per metal atom. These are the oligomers $[\text{Re}(\text{CO})_4\text{H}]_n$ ($n = 2, 3$ or 4) and two anions derived from one of them ($[\text{Re}_3(\text{CO})_{12}\text{H}]^{2-}$ and $[\text{Re}_3(\text{CO})_{12}\text{H}_2]^-$). The parent neutral species can be regarded as analogues of ethene, cyclopropane and cyclobutane respectively in view of the isolobal relationship between the units $\text{Re}(\text{CO})_4\text{H}$ and CH_2 , both of which can make two electrons and two orbitals available for skeletal bonding purposes. Ring strain in the metal oligomers, and metal–metal bond protonation effects are responsible for the differences between $\Sigma E(\text{Re–Re})/x$ over this series of formally similar species. For the neutral species $[\text{Re}(\text{CO})_4\text{H}]_n$, the strongest metal–metal bonding (hydrogen bridged) significantly occurs in the case of the trimer, which can accommodate a presumably preferred H–Re–H angle of 90° better than either the dimer $\text{Re}_2(\text{CO})_8\text{H}_2$ or the tetramer $\text{Re}_4(\text{CO})_{16}\text{H}_4$, as the bridging hydrogen atoms preferably lie off the metal–metal axes.

The rhenium clusters, even more than the osmium clusters discussed above, show a wide range of values of $\Sigma E(\text{Re–Re})/S_{1b}$ though seemingly better suited to localized bond treatments. The value of $\Sigma E(\text{Re–Re})/S_{1b}$ varies from 45 to 85 kJ mol $^{-1}$, a spread that underlines the difficulties of assigning bond enthalpies to skeletal bond pairs, whether as counted in PSEPT (when huge differences are expected depending on the category of cluster, *closo*, *nido*, *arachno*-, etc.) or as counted for localized 2c2e bond schemes compatible with the 18-electron rule (when huge differences are found, though not expected).

8. Rhodium carbonyl clusters, $[\text{Rh}_x(\text{CO})_y\text{H}_z]^{c-}$ and $[\text{Rh}_x(\text{CO})_y\text{H}_z\text{E}]^{c-}$

Rhodium is another metal for which substantial structural information is available in connection with its carbonyl clusters. Most are of formula types $[\text{Rh}_x(\text{CO})_y\text{H}_z]^{c-}$ or $[\text{Rh}_x(\text{CO})_y\text{H}_z\text{E}]^{c-}$ containing a core carbon atom, though examples are also known that contain core nitrogen, phosphorus, arsenic, antimony and sulphur atoms (E) [42], and indeed core rhodium atoms [2]. Unravelling links between their structures and thermochemistry will require more thermochemical information than is available at present, which relates only to the tetranuclear and hexanuclear clusters $\text{Rh}_4(\text{CO})_{12}$ and $\text{Rh}_6(\text{CO})_{16}$ [9,43]. We therefore confine our discussion here to a brief overview.

The known enthalpy of vaporisation of rhodium (556.9 kJ mol $^{-1}$) and inter-atomic distance to nearest neighbour atoms in its face-centred cubic lattice correspond to a bond enthalpy–bond length relationship:

$$E(\text{Rh–Rh}) = 1.396 \times 10^{13} d^{-4.6},$$

Using this relationship and drawing bond lengths from structural databases, we have calculated $\Sigma E(\text{Rh–Rh})$ for some 30 compounds and these are tabulated in Table 6 [44]. We plot the total metal–metal bond enthalpies per metal atom, $\Sigma E(\text{Rh–Rh})/x$, against the total numbers of valence shell electrons per metal atom $(9x + 2y + z + c)/x$ in Fig. 12, identifying the compound type by using different

symbols. Showing less scatter than the rhenium data in Fig. 11, but more than the osmium data in Figs. 4 and 7, the points fall close to a smooth curve that in principle links the atomisation enthalpy of the bulk metal, 556.9 kJ mol⁻¹, to a value of zero at a total of 18 electrons per metal atom. Points corresponding to

Table 6

The carbonyl, carbonyl anion, carbonyl hydride, and carbonyl hydride anion clusters of rhodium, [Rh_x(CO)_yH_z]^{c-} and clusters containing core atoms [Rh_x(CO)_yH_zE]^{c-}, studied, listing the total rhodium–rhodium bond enthalpy (kJ mol⁻¹), and number of ligand electrons (2y + z + c)

Formula	ΣE(Rh–Rh) (kJ mol ⁻¹)	Total ligand electrons 2y + z + c
[Rh ₂₂ (CO) ₃₇] ⁴⁻	5593.6	78
[Rh ₂₂ (CO) ₃₅ H ₂] ^{(6-z)-}	5986.3	76
[Rh ₁₇ (CO) ₃₀] ³⁻	4160.2	66
[Rh ₁₅ (CO) ₂₇] ³⁻	3623.3	57
[Rh ₁₄ (CO) ₂₆] ²⁻	3380.6	54
[Rh ₁₄ (CO) ₂₅] ⁴⁻	3425.9	54
[Rh ₁₄ (CO) ₂₅ H] ³⁻	3404.3	54
[Rh ₁₃ (CO) ₂₄ H] ⁴⁻	2870.1	53
[Rh ₁₃ (CO) ₂₄ H ₂] ³⁻	2853	53
Rh ₁₂ (CO) ₂₅ H ₂	2408.5	52
[Rh ₁₀ (CO) ₂₁] ²⁻	1981.2	44
[Rh ₁₁ (CO) ₂₃] ³⁻	2183.6	49
[Rh ₉ (CO) ₁₉] ³⁻	1740.8	41
[Rh ₇ (CO) ₁₆] ³⁻	1213.4	35
[Rh ₆ (CO) ₁₄] ₂ (μ-CO) ₂	2001.4	60
Rh ₆ (CO) ₁₆	964.6	32
Rh ₄ (CO) ₁₂	520	24
[Rh ₄ (CO) ₁₁] ²⁻	490	24
[Rh ₅ (CO) ₁₅] ⁻	615	31
[Rh ₆ (CO) ₁₅ Cl] ²⁻	712	36
[Rh ₁₂ (CO) ₂₃ (C) ₂] ⁴⁻	2162	58
Rh ₁₂ (CO) ₂₅ (C) ₂	2174.7	58
[Rh ₁₂ (CO) ₂₄ (C) ₂] ²⁻	2207.7	58
[Rh ₁₅ (CO) ₂₈ (C) ₂] ⁻	3028.7	65
[Rh ₆ (CO) ₁₃ Cl] ²⁻	798.8	32
Rh ₈ (CO) ₁₉ C	1160.3	42
[Rh ₁₄ (CO) ₃₃ (C) ₂] ²⁻	2040.8	72
[Rh ₆ (CO) ₁₅ N] ⁻	718.55	36
[Rh ₆ (CO) ₁₄ NH] ²⁻	733.3	36
[Rh ₇ (CO) ₁₅ N] ²⁻	1042.7	37
[Rh ₁₂ (CO) ₂₃ (N) ₂ H] ³⁻	1996.7	60
[Rh ₂₃ (CO) ₃₈ (N) ₄] ⁻	4849.9	97
[Rh ₁₄ (CO) ₂₅ (N) ₂] ²⁻	2779.2	62
[Rh ₂₈ (CO) ₄₁ N ₄ H ₂] ⁴⁻	6577.2	108
[Rh ₉ (CO) ₂₁ P] ²⁻	1274.5	49
[Rh ₁₀ (CO) ₂₂ P] ³⁻	1577.7	52
[Rh ₁₀ (CO) ₂₂ As] ³⁻	1463.8	52
[Rh ₁₇ (CO) ₃₂ (S) ₂] ³⁻	2808.3	81
[Rh ₁₂ (CO) ₂₇ Sb] ³⁻	1830.8	62

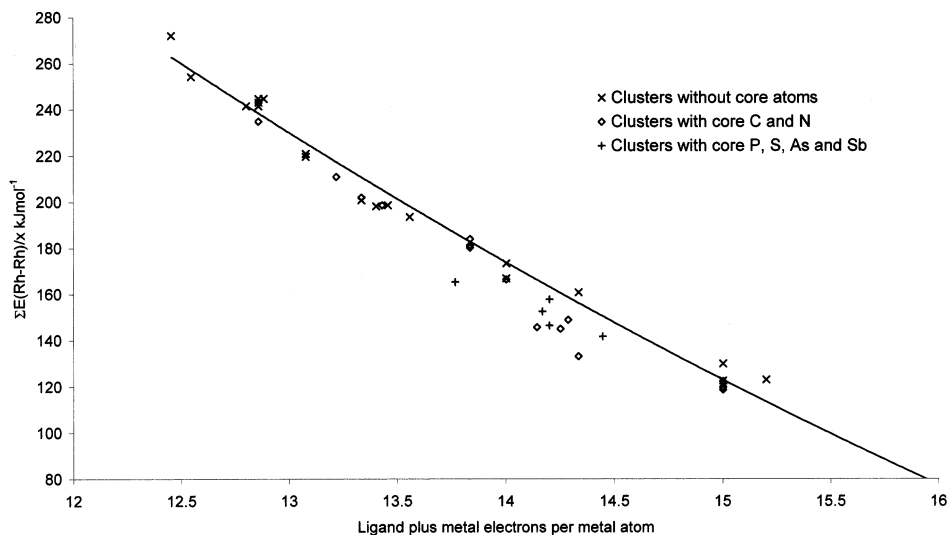


Fig. 12. Plot of $\Sigma E(\text{Rh-Rh})/x$ against the number of ligand plus metal valence shell electrons per metal atom for the three classes of rhodium carbonyl clusters $[\text{Ru}_x(\text{CO})_y\text{H}_z\text{E}]^{c-}$.

carbonyls $[\text{Rh}_x(\text{CO})_y]^{c-}$ and carbonyl hydrides, $[\text{Rh}_x(\text{CO})_y\text{H}_z]^{c-}$, whether neutral ($c = 0$) or anionic, have values of $\Sigma E(\text{Rh-Rh})/x$ that lie within 5 kJ mol^{-1} of the curve that best fits the data. Points corresponding to species containing core carbon or nitrogen atoms generally fall some $5\text{--}10 \text{ kJ mol}^{-1}$ below that curve. The implication of this observation contrasts with that noted above for rhenium carbonyl ‘carbide’ clusters. It is as if in these rhodium systems the core atoms are larger than the cavity size corresponding to the expected metal–metal distances. In the octahedral cluster $[\text{Rh}_6(\text{CO})_{13}\text{C}]^{2-}$ the mean octahedron edge length is 291 pm, implying a Rh atom radius of 145.5 pm, and the cross-octahedron distances average 409 pm. Together these imply a radius of 59 pm for the site occupied by the core carbon atom. Species containing the larger 2nd and 3rd period main group atoms (phosphorus or sulphur and arsenic) have markedly lower values of $\Sigma E(\text{Rh-Rh})/x$ because of the larger metal–metal distances needed to accommodate these larger core atoms.

9. Metal carbides

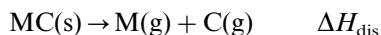
Our discussion of clusters containing core (interstitial) atoms, generally core carbon atoms, so far has focused attention on the effect such core atoms have on the strength of the metal–metal bonding in such clusters, and two factors have been evident. One factor is that, by providing all of their valence shell electrons (four in the case of carbon) towards the total number of electrons accessible to the metal atoms in these clusters, such core carbon atoms affect the strength of the metal–

metal bonding in a similar manner to ligand molecules. The strength of the metal–metal bonding, expressed as $\Sigma E(\text{M–M})/x$, reflects the number of electrons per metal atom in a systematic way as illustrated by Figs. 4, 7, 11 and 12. The second way in which core atoms may affect the strength of the metal–metal bonding is effectively steric; by holding the metal atoms at the optimum distance for bonding to the core atom, they may increase or decrease the metal–metal distances, and so the strength of the metal–metal bonds, relative to the values expected from the electron count.

In considering these clusters containing core carbon atoms, we have been unable to assign bond enthalpies to their metal–carbon bonds because thermochemical measurements have not, to our knowledge, been made yet of cluster compounds containing such core carbon atoms. However, some indication of the likely strength of the metal–carbon bonds in such systems can, in principle, be obtained by reference to extended lattices containing carbon atoms in similar metal environments, i.e. by a consideration of metal carbides M_aC_b , many of which have been characterised thermochemically [45] and structurally.

Transition metal carbides include a number of extremely important materials [46]. Substances like tungsten carbide, WC, are among the hardest known materials (which in itself gives a qualitative indication of the strength of their metal–carbon bonds), and indeed the capacity of carbon to toughen metals has been known since the earliest days of steel-making. However, difficulties with the preparation of stoichiometric metal carbides of established structures and thermochemistry have affected the quantity and quality of information about such materials. The metals of most interest to us here, osmium, rhenium and rhodium are not known to form thermodynamically stable binary carbide phases, M_aC_b , and the carbides of the 3d metals in the same groups as these metals have very complicated structures. However, enough is known about the carbides of early transition metals to provide some useful pointers.

Metal carbides contain metal atoms at distances $d(\text{M–M})$ similar to those in the bulk metals. Moreover, they function as metallic conductors of electricity. It seems appropriate therefore, to treat their metal–metal bonding in the same way that we have used here for bulk metals or metal clusters, by assigning enthalpies to neighbouring metal–metal bonding contacts. We suggest that the enthalpy of disruption of a metal carbide into gaseous metal and carbon atoms,



$$\Delta H_{\text{dis}} = \Delta_f H(\text{M(g)}) + \Delta_f H(\text{C(g)}) - \Delta_f H(\text{MC(s)})$$

can be expressed as the sum of two bond enthalpy terms, $\Sigma E(\text{M–M})$ and $\Sigma E(\text{M–C})$, referring to the metal–metal and metal–carbon bonds, respectively. We ignore carbon–carbon bonding interactions as negligible in view of their lengths (equal to the metal–metal distances in metal carbides MC that have the rock-salt structure, as is known to be the case for the carbides of the titanium, vanadium and chromium sub-groups). Thus:

$$\Delta H_{\text{dis}} = \Sigma E(\text{M–M}) + \Sigma E(\text{M–C})$$

For metal carbides of known structure and enthalpy of formation, we can calculate $\Sigma E(\text{M-M})$ in the usual way from the metal–metal distances $d(\text{M-M})$, subtract it from the disruption enthalpy ΔH_{dis} (itself calculated from the enthalpies of formation of the metal carbide and of gaseous metal and carbon atoms) and so deduce $\Sigma E(\text{M-C})$.

Such calculations have been carried out for carbides MC and M_2C formed by early transition metals of the titanium, vanadium and chromium groups [47]. Data for such species are listed in Table 7. For all of these systems, the values of $\Sigma E(\text{M-C})$, which may be regarded as the enthalpy change associated with the cleavage of the six octahedrally-orientated metal–carbon bonds that hold the core carbon atoms in place in these compounds (the ‘carbide’ carbon atoms occupy octahedral holes in the metal lattices in most of these cases, though trigonal prismatic carbon sites are found in WC) lie in the range 1000–1280 kJ mol^{−1}, and vary by 40 to 110 kJ mol^{−1} within a sub-group. It requires more energy to break the shorter metal–carbon bonds in a species M_2C than it does to break the longer metal–carbon bonds in a species MC. The strength of the metal–carbon bonds in these systems, as represented by $\Sigma E(\text{M-C})$, exceeds that of the metal–metal bonds, represented by $\Sigma E(\text{M-M})$, in all cases (including phases of composition M_2C) except for W_2C . These observations are consistent with the known mechanical hardness and refractory nature of these materials, and echo suggestions made 50 years ago by Pauling on the basis of an analysis of the bonding in cementite, Fe_3C [48]. The mechanical properties of transition metal carbides clearly reflect the strength of their metal–carbon bonds.

Comparison of the data for species MC and M_2C shows that $\Sigma E(\text{M-M})/x$, the total metal–metal bond enthalpy per mole of metal, increases from MC to M_2C , reflecting the shorter, stronger metal–metal bonds in the latter. Both stoichiometries can be regarded as having close-packed metal lattices expanded to incorporate the (interstitial) carbon atoms, the expansion being greater in MC than in M_2C . As noted above, the M–C bonds in M_2C are shorter than those in MC, and this is reflected in the greater values of $\Sigma E(\text{M-C})$ for the former.

The data in Table 7 incidentally correspond to a radius for the octahedrally coordinated carbon atom that varies from ca. 59 to 69 pm (determined by taking half the metal–metal distance as being the metal radius and subtracting this from the metal–carbon distance). We have already noted that, in the rhenium carbonyl carbide, $[\text{Re}_6(\text{CO})_{19}\text{C}]^{2-}$, the effective radius of the carbon atom is 62 pm, that in the rhodium cluster $[\text{Rh}_6(\text{CO})_{13}\text{C}]^{2-}$, the radius of the carbon atom is approximately 59 pm, and that in the $[\text{Os}_{10}(\text{CO})_{24}\text{H}_z\text{C}]^{(2-z)-}$ series of clusters ($z = 0, 1, 2$) the radius of the carbon atom approximates to 60 pm. It seems likely that the enthalpy change, $\Sigma E(\text{M-C})$, needed to cleave the six M–C bonds in such a metal carbonyl carbide cluster will lie in the same range (1000–1300 kJ mol^{−1}) as we have calculated for the similarly coordinated carbon atoms of the binary carbides MC or M_2C . Ultimately, we hope to be able to express the disruption enthalpy, ΔH_{dis} , of a metal carbonyl carbide $[\text{M}_x(\text{CO})_y\text{C}]$ into metal and carbon atoms and carbon monoxide molecules:

Table 7
Calculated contributions to the enthalpy of disruption of selected metal carbides

	M–M distance in MC (pm)	$\Sigma E(\text{M–M})$ in MC (kJ mol^{-1})	$\Delta_f H$ of MC (kJ mol^{-1})	$\Delta H_{\text{disrupt}}$ (kJ mol^{-1})	$\Sigma E(\text{M–C})$ (kJ mol^{-1})	M–C distance (pm)	% age of bonding contributed by $E(\text{M–C})$
TiC	306.0	364.4	–184	1370.6	1006.2	216.4	73.4
ZrC	332.2	497.3	–203	1528.5	1031.2	234.9	67.5
HfC	328.1	496.4	–209.5	1545.2	1048.8	232.0	67.9
VC _{0.88}	295.2	322.6	–101.9	1236.8	914.2	208.75	73.9
NbC	316.1	491.8	140.6	1613.2	1121.4	223.5	69.5
TaC	315.1	544.5	–148.1	1646.7	1102.2	222.8	66.9
V ₂ C	290.2, 283.6	736.9	–147.2	1892.3	1155.4	202.9	61.1
Nb ₂ C	312.7, 307.2	1077.7	–195.5	2364.0	1286.3	219.2	54.4
Ta ₂ C	310.6, 305.4	1210.5	–197.5	2478.2	1267.7	217.8	51.2
Mo ₂ C	301.1, 295.2	940.4	–53.1	2086.0	1145.6	210.8	54.9
W ₂ C	299.3, 292.8	1296.6	–26.4	2444.1	1144.5	209.3	46.9

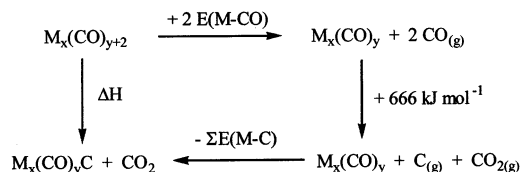


in the form

$$\Delta H_{\text{dis}} = \Sigma E(M-M) + \Sigma E(M-CO) + \Sigma E(M-C)$$

where $\Sigma E(M-C)$ is calculated from binary carbide data for the metal in question.

Assuming that $\Sigma E(M-C)$ for metal carbonyl clusters does in fact lie in the range 1000–1300 kJ mol⁻¹, we are in a position to consider the enthalpy change associated with the formation of a metal carbonyl carbide $M_x(CO)_yC$ from a cluster carbonyl precursor $M_x(CO)_{y+2}$ by loss of carbon dioxide. Setting up a thermal cycle as follows



one calculates the enthalpy change, ΔH , for the reaction:



to be

$$\Delta H = 2 E(M-CO) + 666 - \Sigma E(M-C)$$

This will be positive (exothermic) for osmium, for which $E(M-CO)$ is ca. 200 kJ mol⁻¹, if $\Sigma E(M-C)$ exceeds ca. 1070 kJ mol⁻¹. As $M_x(CO)_{y+2}$ and $M_x(CO)_yC$ are isoelectronic we expect only a small difference in the values of $\Sigma E(M-M)$ for these two clusters, as a consequence of the need to accommodate the core carbon atom; for osmium this will be of the magnitude observed in Table 5.

We are carrying out a detailed analysis of the limited data available for carbides of transition metals further to the right in the d-block than those in Table 7, in order to gain some feeling for the strength of binding of carbon atoms octahedrally coordinated by metal atoms, and so to gain further insight into the bonding and thermochemistry of metal carbonyl clusters containing core carbon atoms. In order to probe the thermodynamics of clusters containing core ‘nitride’ atoms, we are also carrying out an analysis of the thermochemistry and structures of binary metal nitrides, MN and M₂N, known for the early transition metals.

10. Conclusions

In this review, we have explored the extent to which the now huge and steadily accumulating amount of information about the structures of metal carbonyl and metal carbonyl hydride cluster compounds of general formulae $[M_x(CO)_yH_z]^{c-}$, and of related clusters containing an atom of carbon or some other element E at their core, $[M_x(CO)_yH_zE]^{c-}$, can be correlated with the far more limited amount of

experimental thermochemical information about such clusters. By assuming that the metal–metal bonds in these clusters resemble those in the bulk metal, and that they vary consistently in strength with length, it had been shown possible some 20 years ago to deduce metal–ligand bond enthalpy terms, $E(\text{M}–\text{CO})$, for some neutral carbonyl clusters $\text{M}_x(\text{CO})_y$ of the iron and cobalt groups that were in line with the known heats of disruption of carbon monoxide from metal surfaces, and that varied with cluster nuclearity in a manner that makes sense in terms of competition between ligands for metal sites and electrons, a variation that has subsequently been shown to be supported by subtle variations with nuclearity in the metal–carbon and carbon–oxygen bond distances in such systems.

Encouraged by that, we have explored what trends become apparent, even for systems that have not been thermochemically characterised, in the metal–metal bonding in clusters as the numbers and types of ligands are varied. Focusing initially on the most fully documented series of metal carbonyl clusters, those of osmium, we have shown that the calculated strengths per metal atom of their metal–metal bonds, when plotted against the total numbers of electrons available to the metal valence shells, generates a smooth curve that can be extrapolated to the bond strength in osmium metal itself, and that shows that, as ligand demands for metal orbitals (and number of electrons available) decrease, so the remaining electrons are used progressively more effectively for metal–metal bonding. The good fit to the curve of points corresponding to neutral or anionic cluster carbonyls and carbonyl hydrides, $[\text{Os}_x(\text{CO})_y\text{H}_z]^{e-}$, and indeed to systems containing other ligands, allows the strength of metal–metal bonding in other clusters yet to be structurally characterised to be predicted from their electron counts.

Similar correlations between calculated metal–metal bond enthalpies and electron numbers have been found for rhenium and rhodium systems, though the data show more scatter than for osmium, largely because we have included data for core carbon, and other, atoms occupying holes (usually octahedral) in the cluster polyhedra. Such carbon atoms, because of their size and the strength of the metal–carbon bonds they form, can distort (reduce or increase) the interatomic distances between the metal atoms and so perturb them from the values their electron counts would lead one to expect. Bridging hydride ligands have a similar capacity to affect metal–metal distances and implied skeletal bond energies.

In a later section, we showed how some insight into the strength of binding of such core carbon atoms themselves might be obtained by reference to binary metal carbides, though published information on the carbides of osmium, rhenium and rhodium, those of most interest to us at present, is scarce. Nevertheless some useful pointers were provided by data on early transition metal carbide systems.

To conclude: from the data currently available it is possible to make realistic estimates of bond enthalpies for the metal–metal and metal–ligand bonds in an expanding series of metal–cluster compounds, including those containing core atoms. However, there remains an urgent need to carry out more experimental work, to document more thoroughly the thermochemistry of such systems, in order to allow predictions based on structural data to be tested.

Acknowledgements

We acknowledge the contributions made to this work by our co-workers, in the early phase of this work these were Catherine Housecroft, Marion O'Neill, and Barry Smith; more recently we have worked with Karen Peat, Kate Hillary, Lyndsey Rabbitt and Andrew Johnson. Financial support has been given by EPSRC and Kvaerner Process Technology through the CASE scheme. Structural data have been retrieved from the Cambridge Structural Database [3], and the Inorganic Crystal Structure Database using the EPSRCs Chemical Database Service at Daresbury [49].

References

- [1] (a) M.P. Cifuentes, M.G. Humphrey, in: E.W. Abel, F.G.A. Stone, G. Wilkinson (Eds.), *Comprehensive Organometallic Chemistry II*, vol. 7, Pergamon, Oxford, 1995 (Chapter 16). (b) B.F.G. Johnson, J. Lewis, *Adv. Inorg. Chem. Radiochem.* 24 (1981) 225.
- [2] C.E. Barnes, in: E.W. Abel, F.G.A. Stone, G. Wilkinson (Eds.), *Comprehensive Organometallic Chemistry II*, vol. 8, Pergamon, Oxford, 1995 (Chapter 4).
- [3] F.H. Allen, O. Kennard, *Chem. Des. Autom. News* 8 (1993) 1 and 31.
- [4] S.M. Owen, *Polyhedron* 7 (1988) 253.
- [5] (a) M. McPartlin, *Polyhedron* 3 (1984) 1279. (b) M. McPartlin, D.M.P. Mingos, *Polyhedron* 3 (1984) 1321.
- [6] K. Wade, *Adv. Inorg. Chem. Radiochem.* 18 (1976) 1.
- [7] C.E. Housecroft, K. Wade, *Gazz. Chim. Ital.* 110 (1980) 87.
- [8] (a) J.A. Connor, *Top. Curr. Chem.* 71 (1977) 71. (b) H.A. Skinner, *J. Chem. Thermodyn.* 10 (1978) 309. (c) G. Pilcher, H.A. Skinner, in: F.R. Hartley, S. Patai (Eds.), *The Chemistry of the Metal–Carbon Bond*, vol. 1, Wiley, Chichester, 1982. (d) S.P. Nolan, *Bonding energetics of organometallic compounds*, in: R.B. King (Ed.), *Encyclopedia of Inorganic Chemistry*, Wiley, Chichester, 1994. (e) J.A. Martinho Simoes, J.L. Beauchamp, *Chem. Rev.* 90 (1990) 629. (f) J.A. Connor, in: B.F.G. Johnson (Ed.), *Transition Metal Clusters*, Wiley, Chichester, 1980 (Chapter 5).
- [9] J.A. Connor, H.A. Skinner, Y. Virmani, *Faraday Symp. Chem. Soc.* 8 (1973) 18.
- [10] S.L. Morrison, J.J. Turner, *J. Mol. Struct.* 317 (1994) 39.
- [11] L. Pauling, *The Nature of the Chemical Bond*, third ed., Cornell University Press, Ithaca, NY, 1960.
- [12] However, we are aware of at least one case where longer bonds are associated with apparently greater metal–ligand binding energies, as determined by the enthalpy change associated with ligand exchange in a coordinating solvent; R.D. Ernst, J.W. Freeman, L. Stahl, D.R. Wilson, A.M. Arif, B. Nuber, M.L. Ziegler, *J. Am. Chem. Soc.* 117 (1995) 5075.
- [13] (a) I.D. Brown, R.D. Shannon, *Acta Crystallogr. Sect. A* 29 (1973) 266. (b) O. Sulpecki, I.D. Brown, *Acta Crystallogr. Sect. B* 38 (1982) 1078. (c) I.D. Brown, D. Altermatt, *Acta Crystallogr. Sect. B* 41 (1985) 244. (d) N.E. Brese, M. O'Keeffe, *Acta Crystallogr. Sect. B* 47 (1991) 192. (e) M. O'Keeffe, N.E. Brese, *Acta Crystallogr. Sect. B* 48 (1992) 152. (f) I.D. Brown, *Acta Crystallogr. Sect. B* 48 (1992) 553. (g) M. O'Keeffe, *Struct. Bonding* 71 (1989) 161.
- [14] For some extensions of the bond valence method to thermodynamic measures of bond strength see: (a) J. Ziolkowski, *J. Solid State Chem.* 57 (1985) 269. (b) M. O'Keeffe, J.A. Stuart, *Inorg. Chem.* 22 (1983) 177.
- [15] D.A. Johnson, *Some Thermodynamic Aspects of Inorganic Chemistry*, second ed., Cambridge University Press, Cambridge, 1982 (Chapter 7).

- [16] S. Parsons, J. Passmore, *Inorg. Chem.* 31 (1992) 526.
- [17] (a) S.W. Benson, *J. Chem. Educ.* 42 (1965) 502. (b) S.W. Benson, F.R. Cruickshank, D.M. Golden, G.R. Haugen, H.E. O'Neal, A.S. Rodgers, R. Shaw, R. Walsh, *Chem. Rev.* 69 (1969) 279.
- [18] (a) J. March, *Advanced Organic Chemistry*, third ed., Wiley, Chichester, 1985, p. 23 and Refs. therein. (b) J.G. Stark, H.G. Wallace, *Chemistry Data Book*, second ed., John Murray Ltd., London, 1982, p. 32.
- [19] Tables of Interatomic distances and configurations in molecules and ions, L.E. Sutton (Ed.), *Chem. Soc. Spec. Publ. No. 11*, 1958.
- [20] For some examples of experimental thermochemical studies on metal carbonyl complexes: (a) A.J. Poë, C.N. Sampson, R.T. Smith, Y. Zheng, *J. Am. Chem. Soc.* 115 (1993) 3174. (b) G. Bor, U.K. Dietler, *J. Organomet. Chem.* 191 (1980) 295. (c) F. Oldani, G. Bor, *J. Organomet. Chem.* 246 (1983) 309. (d) M. Garland, I.T. Horváth, G. Bor, P. Pino, *Organometallics* 10 (1991) 559.
- [21] K. Wade, *Inorg. Nucl. Chem. Lett.* 14 (1978) 71.
- [22] C.E. Housecroft, K. Wade, B.C. Smith, *J. Chem. Soc. Chem. Commun.* (1978) 766.
- [23] C.E. Housecroft, M.E. O'Neill, K. Wade, B.C. Smith, *J. Organomet. Chem.* 213 (1981) 35.
- [24] (a) R.G. Behrens, *J. Less Common Met.* 56 (1977) 55. (b) R.G. Behrens, *J. Less Common Met.* 58 (1978) 47.
- [25] (a) D. Brennan, F.H. Hayes, *Phil. Trans. Roy. Soc. A* 258 (1965) 347. (b) R.W. Joyner, M.W. Roberts, *Chem. Phys. Lett.* 29 (1974) 447. (c) W. Biemolt, A.P.J. Jansen, *J. Comput. Chem.* 10 (1994) 1053.
- [26] A.K. Hughes, K.L. Peat, K. Wade, *J. Chem. Soc. Dalton Trans.* (1996) 4639.
- [27] D. Braga, T.F. Koetzle, *J. Chem. Soc. Chem. Commun.* (1987) 144.
- [28] S.F.A. Kettle, E. Diana, R. Rossetti, P.L. Stanghellini, *J. Am. Chem. Soc.* 119 (1997) 8228.
- [29] C. Elschenbroich, A. Salzer, *Organometallics — A Concise Introduction*, VCH, Weinheim, 1989, p. 230.
- [30] C.E. Housecroft, K. Wade, B.C. Smith, *J. Organomet. Chem.* 170 (1979) C1.
- [31] (a) B.F.G. Johnson, R.E. Benfield, in: B.F.G. Johnson (Ed.), *Transition Metal Clusters*, Wiley, Chichester, 1980 (Chapter 7). (b) B.E. Mann, *J. Chem. Soc. Dalton Trans.* (1997) 1457. (c) B.F.G. Johnson, *J. Chem. Soc. Dalton Trans.* (1997) 1473.
- [32] M.E. Minas de Piedade, J.A. Martinho Simoes, *J. Organomet. Chem.* 518 (1996) 167.
- [33] A.K. Hughes, K.L. Peat, K. Wade, *J. Chem. Soc. Dalton Trans.* (1997) 2139.
- [34] (a) A.G. Orpen, *J. Chem. Soc. Dalton Trans.* (1980) 2509. (b) G. Ciani, D. Gusto, M. Manassero, A. Albinati, *J. Chem. Soc. Dalton Trans.* (1976) 1943. (c) L.H. Gade, B.F.G. Johnson, J. Lewis, *Croat. Chem. Acta* 68 (1995) 683.
- [35] P.F. Jackson, B.F.G. Johnson, J. Lewis, M. McPartlin, W.J.H. Nelson, *J. Chem. Soc. Chem. Commun.* (1980) 224.
- [36] (a) P.F. Jackson, B.F.G. Johnson, J. Lewis, M. McPartlin, W.J.H. Nelson, *J. Chem. Soc. Chem. Commun.* (1982) 49. (b) P.J. Bailey, L.H. Gade, B.F.G. Johnson, J. Lewis, *Chem. Ber.* 125 (1992) 2019.
- [37] D. Braga, F. Grepioni, S. Righi, B.F.G. Johnson, P. Frediani, M. Bianchi, F. Piacenti, J. Lewis, *Organometallics* 11 (1992) 706.
- [38] K.M. Hillary, A.K. Hughes, K.L. Peat, K. Wade, *Polyhedron* 17 (1998) 2803.
- [39] (a) F. Scherbaum, A. Grohmann, B. Huber, C. Kruger, H. Schmidbaur, *Angew. Chem. Int. Ed. Engl.* 27 (1988) 1544. (b) F.P. Gabbai, A. Schier, J. Riede, H. Schmidbaur, *Chem. Ber.* 130 (1997) 111.
- [40] J. Mason, *J. Am. Chem. Soc.* 113 (1991) 24.
- [41] M. Kaupp, *J. Chem. Soc. Chem. Commun.* (1996) 1141.
- [42] J.N. Nicholls, *Polyhedron* 3 (1984) 1307.
- [43] D.L.S. Brown, J.A. Connor, H.A. Skinner, *J. Chem. Soc. Faraday Trans. I* 71 (1975) 699.

- [44] A.K. Hughes, K.L. Peat, K. Wade, manuscript in preparation.
- [45] (a) R.G. Colters, *Mat. Sci. Eng.* 76 (1985) 1. (b) L.E. Noth, *Transition Metal Carbides, Nitrides*, Academic Press, New York, 1971. (c) S.V. Meschel, O.J. Kleppa, *J. Alloy. Compd.* 257 (1997) 227.
- [46] A. Cottrell, *Chemical Bonding in Transition Metal Carbides*, Institute of Materials, London, 1995.
- [47] A.K. Hughes, K. Wade, manuscript in preparation.
- [48] L. Pauling, *J. Am. Chem. Soc.* 69 (1947) 542.
- [49] R.F. McMeeking, D.J. Parkin, *J. Chem. Inf. Comput. Sci.* 36 (1996) 746.